Contemporary Mathematics
https://ojs.wiserpub.com/index.php/CM/

Research Article

A Modified Laplace Fractional Residual Power Series Technique for Handling Non-linear Models of Fuzzy Partial Differential Equations of Fractional Order

Mohammad Alaroud[1], Nedal Tahat[2], A. K. Alomar[3*]

[1] Department of Mathematics, Faculty of Science, Yarmouk University, Irbid, 211-63, Jordan
[2] Department of Mathematics, Faculty of Science, The Hashemite University, Zarqa, 13133, Jordan
[3] Department of Mathematics, Faculty of Science, Islamic University of Madinah, Madinah, 42351, Saudi Arabia
E-mail: abdomari2008@yahoo.com

Received: 15 August 2025; **Revised:** 18 September 2025; **Accepted:** 14 October 2025

Abstract: In this work, the time-nonlinear fuzzy fractional order partial differential equations with a suitable fuzzy initial data in the presence of the Caputo differential operator are analytically and numerically investigated using the extended Laplace fractional residual power series scheme. The analytic-approximate fuzzy solutions have been extracted under generalized Hukuhara partial differentiability via fuzzy Laplace transform, along with the simulation of the fractional residual power series strategy. The suggested approach is demonstrated to be effective in solving three non-linear fractional-order initial value problems under uncertainty; the graphical and numerical impacts demonstrate the algorithm's accuracy and ability. Quantitative and graphical presentations of the influence of fractional-motion and uncertain levels demonstrate the agreement between the fuzzy exact and approximate solutions. The outcomes reveal that the congruence between the lower and upper portions of uncertain levels depictions of the fuzzy solutions, and the convex symmetric triangular fuzzy number is fulfilled. As a result, the proposed scheme is a practical and straightforward mathematical instrument for obtaining fuzzy approximation and exact analytical solutions to time-nonlinear Fuzzy Fractional Order Partial Differential Equations (FFOPDEs) of the specified type.

Keywords: Fuzzy Fractional Order Partial Differential Equations (FFOPDEs), generalized Hukuhara partial differentiability, Laplace fractional residual power series method

MSC: 35A35, 65R10, 34A07

1. Introduction

Fractional Calculus (FC) has been the tractable subject of numerous studies in recent decades since it is frequently used in various fields, including engineering, economics, biology, physics, financial markets, signal processing, and viscoelasticity [1–4]. Over the development of FC theory, Fractional Derivatives (FDs) have been defined in a variety of approaches to describe the behavior of several phenomena structures, including Riemann-Liouville, Caputo, Caputo-Fabrizio FD, and conformable FD. Fractional Order Partial Differential Equations (FOPDEs) are among their most significant uses since they may be used to model most natural phenomena. Due to the widespread usage of FOPDEs

DOI: https://doi.org/10.37256/cm.6620258268

in scientific and engineering applications, numerous researchers in this area have produced novel findings using both theoretical and applied investigation techniques [5–8]. Even so, we can't be certain that these models are perfect, and the information about them is covered by uncertainty in some circumstances. This ambiguity or uncertainty can arise in a variety of ways that can be ascribed to different sources. To beat this problem, Zadeh [9] in 1965 combined the fuzzy set theory with Ordinary Differential Equations (ODEs) to be an efficient tool for modeling this uncertainty, as it can represent imprecision and vagueness. Several researchers used the notions of fuzzy mapping and control to create ordinary fuzzy calculus, including work on the definition of fuzzy numbers and their use in fuzzy control [10] and reasoning about approximate problems [11, 12]. In data analysis, it is challenging to effectively represent several cases with real numbers. Following that, several significant works on the topic of developing the basic arithmetic for fuzzy numbers were conducted [13–16].

The concept of investigating Fuzzy Fractional Order Differential Equations (FFODEs) was initially introduced in 2010 [17] as a tool to model specific real-life situations while accounting for data uncertainty. Possible combinations of the aforementioned FDs and others, along with the notion of fuzzy derivatives, have led to the introduction of various forms of fuzzy FDs, which have been used to investigate FFODEs. Extensive studies have been conducted on FFODEs and Fuzzy Fractional Order Partial Differential Equations (FFOPDEs) in the physical sciences. The solution principle of these equations has been explored [18], and then the existence and uniqueness of solutions to such equations under the initial data have been proven in some cases [19]. Additionally, the existence and uniqueness of FFOPDEs have been investigated in [20], and Laplace Transforms (LTs) have been utilized to simplify these equations and obtain closed-form solutions [21, 22], thereby enhancing the potential of FFOPDEs for practical applications.

Sometimes, nonlinear FFOPDE problems cannot be solved analytically; therefore, obtaining accurate approximate solutions using numerical approaches is quite valuable. In recent times, numerous researchers have devoted their attention to examining solutions to FFOPDEs, employing distinct numerical and analytical techniques that several researchers have effectively utilized to develop algorithms for handling such fractional models.

In this context, the fuzzy fractional Navier-Stokes equations had been solved via the fuzzy Adomian Decomposition Method (ADM) and fuzzy Modified Laplace Decomposition Mthod (MLDM) [23]. Stepnicka and Valasek utilized the Fuzzy Transform Method (FTM) to solve the finite fuzzy wave problem [24]. In [25], the fuzzy solution of the heat equation was introduced by applying the Fuzzy Fractional Transform (FFT). The fuzzy LT, along with ADM, had been used to obtain general numerical findings for a complex population dynamical model [26]. Allahviranloo et al. [27] suggested Fuzzy Fourier Sine Transform (FFST) of a fuzzy wave equation in the meaning of generalized Hukuhara partial differentiability (gH-partial differentiability). The authors of [28, 29] have promoted the work of [30–32] by using the ADM to examine numerical findings of a particular class of nonlinear FFOPDEs in the context of a fuzzy environment.. Motivated by the works mentioned above, the LT simplifies the treatment of FDs by reducing convolution-type processes and exhibiting a high convergence rate among different transform techniques. Additionally, by methodically reducing truncation errors, the Fractal Residual Power Series (FRPS) framework accelerates convergence and often requires fewer terms for adequate accuracy. Since no iterative correction functions or auxiliary parameters are required, unlike the Adomian Decomposition Method (ADM), Homotopy Analysis Method (HAM), and the Variational Iteration Method (VIM) [33–35], implementation is straightforward. Overall, the computational efficiency of the Laplace-Fractional Residual Power Series method (L-FRPS) is notably superior to that of several existing analytical methods. Unlike the Laplace Decomposition Method, which performs iterative transformations, the L-FRPS scheme computes the inverse LT only once. It also avoids the need to evaluate an inverse linear operator at each step, as required by ADM. Moreover, the L-FRPS eliminates the convergence-control parameters essential to HAM, whose optimization is computationally expensive. Finally, it provides a straightforward recurrence relation for series terms, a feature absent in the standard FRPS approach. These factors contribute to the significantly lower computational expense of the proposed algorithm, where it maintains competitive accuracy when compared to the existing approaches while combining simplicity and efficiency for a variety of nonlinear FFOPDEs. We aim in the present investigation to use fuzzy LT along with the FRPS algorithm to generate accurate approximate solutions of certain time-nonlinear FFOPDEs in light of fuzzy Caputo differentiability.

The article is structured as follows: In Section 2, we present an overview of fuzzy FC theory. As for Section 3, certain basic preliminary results concerning the fuzzy LT tool and the L-FRPS scheme are provided, as well as the framework of the methodology of the suggested algorithm for extracting FPS solutions. The computed findings and numerical implementations are presented in Section 4. To end, Section 5 presents the concluding remarks.

2. Preliminaries

This section highlights essential characteristics related to FC and fuzzy set theories, as well as critical findings about the LFRPS method. In [36], a fuzzy number is defined as a fuzzy subset of the real line. Any fuzzy number can be conceived of as a function whose domain is a certain set, i.e., we call $\Lambda : \mathbb{R} \to [0,\ 1]$, is a fuzzy number if it holds the following assumptions:

a) Λ is upper semi-continuous, i.e. $\lim_{\tau \to \vartheta} \Lambda(\tau) \geq \Lambda(\vartheta),\ \forall \vartheta \in \mathbb{R}$.

b) Λ is normal, i.e., there is at least one point $\vartheta \in \mathbb{R}$ such that $\Lambda(\vartheta) = 1$.

c) Λ is convex, i.e., for each $\vartheta_1,\ \vartheta_2 \in \mathbb{R}$, and $0 \leq v \leq 1$, we have $\Lambda(v\vartheta_1 + (1-v)\vartheta_2) \geq \min(\Lambda(\vartheta_1),\ \Lambda(\vartheta_2))$.

d) $\operatorname{supp}(\Lambda) = \{\vartheta \in \mathbb{R} : \Lambda(\vartheta) > 0\}$ is the support of Λ and its closure is a compact set.

Assume that $\mathbb{F}_{\mathbb{R}}$ is the set of all fuzzy numbers on $\mathbb{R}$. The parametric form representation of a fuzzy number $\Lambda \in \mathbb{F}_{\mathbb{R}}$ can be described as $[\Lambda]_{\varsigma} = \{\vartheta \in \mathbb{R} \mid \Lambda(\vartheta) \geq \varsigma\} = [\underline{\Lambda}(\varsigma),\ \overline{\Lambda}(\varsigma)]$ for $\varsigma \in [0,\ 1]$.

Defintion 2.1 [13] For $\varsigma \in [0,\ 1]$, the parametric form $[\underline{\Lambda}(\varsigma),\ \overline{\Lambda}(\varsigma)]$, fulfills the following presumptions:

a) $\overline{\Lambda}(\varsigma)$ is a bounded, non-increasing, left-continuous function in $(0,\ 1]$, and right continuous at 0,

b) $\underline{\Lambda}(\varsigma)$ is a bounded, non-decreasing, left-continuous function in $(0,\ 1]$, and right continuous at 0,

c) $\underline{\Lambda}(\varsigma) \leq \overline{\Lambda}(\varsigma)$.

Defintion 2.2 [13] Let $[\Lambda]_{\varsigma} = [\underline{\Lambda}(\varsigma),\ \overline{\Lambda}(\varsigma)]$ and $[\Theta]_{\varsigma} = [\underline{\Theta}(\varsigma),\ \overline{\Theta}(\varsigma)]$, be two arbitrary fuzzy numbers and $\lambda \in \mathbb{R}$. Then we have the following arithmetic operations:

a) $[\Lambda + \Theta]_{\varsigma} = [\Lambda]_{\varsigma} + [\Theta]_{\varsigma} = [\underline{\Lambda}(\varsigma) + \underline{\Theta}(\varsigma),\ \overline{\Lambda}(\varsigma) + \overline{\Theta}(\varsigma]$,

b) $[\Lambda - \Theta]_{\varsigma} = [\Lambda]_{\varsigma} - [\Theta]_{\varsigma} = [\underline{\Lambda}(\varsigma) - \underline{\Theta}(\varsigma),\ \overline{\Lambda}(\varsigma) - \overline{\Theta}(\varsigma]$

c) $\lambda[\Lambda]_{\varsigma} = [\min\{\lambda\underline{\Lambda}(\varsigma),\ \lambda\overline{\Lambda}(\varsigma)\},\ \max\{\lambda\underline{\Lambda}(\varsigma),\ \lambda\overline{\Lambda}(\varsigma)\}]$.

Definition 2.3 [14] Given two fuzzy numbers $\Lambda,\ \Theta \in \mathbb{F}_{\mathbb{R}}$. The generalized Hukuhara difference ($g\mathcal{H}$-difference) is defined as the fuzzy number $\Xi \in \mathbb{F}_{\mathbb{R}}$ such that

$$\Lambda \ominus_{g\mathcal{H}} \Theta = \Xi \Leftrightarrow \begin{cases} \text{(i) } \Lambda = \Theta + \Xi \ \text{ or} \\ \\ \text{(ii) } \Theta = \Lambda + (-1)\Xi. \end{cases}$$

Definition 2.4 [14] Assume that $\Upsilon : [a,\ b] \to \mathbb{F}_{\mathbb{R}}$, then the $g\mathcal{H}$-partial derivative of first-order at the point $(\vartheta_0,\ \zeta_0)$ is denoted by $\partial^{\vartheta}_{g\mathcal{H}}\Upsilon(\vartheta_0,\ \zeta_0),\ \partial^{\zeta}_{g\mathcal{H}}\Upsilon(\vartheta_0,\ \zeta_0)$, and given by

$$\partial_{\vartheta_{g\mathcal{H}}}\Upsilon(\vartheta_0,\ \zeta_0) = \lim_{h_1 \to 0^+} \frac{\Upsilon(\vartheta_0 + h,\ \zeta_0) \ominus_{g\mathcal{H}} \Upsilon(\vartheta_0,\ \zeta_0)}{h},$$

$$\partial_{\zeta_{g\mathcal{H}}}\Upsilon(\vartheta_0,\ \zeta_0) = \lim_{h_2 \to 0^+} \frac{\Upsilon(\vartheta_0,\ \zeta_0 + k) \ominus_{g\mathcal{H}} \Upsilon(\vartheta_0,\ \zeta_0)}{k},$$

provided that $\partial_{\vartheta_{g\mathcal{H}}}\Upsilon(\vartheta_0,\ \zeta_0),\ \partial_{\zeta_{g\mathcal{H}}}\Upsilon(\vartheta_0,\ \zeta_0) \in \mathbb{F}_{\mathbb{R}}$.

Definition 2.5 [32] Assume that $\Upsilon(\vartheta,\ \zeta;\ \varsigma) \in \mathbb{F}_{\mathbb{R}},\ (\vartheta_0,\ \zeta_0) \in [a,\ b]$ with respect to ζ and $\underline{\Upsilon}(\vartheta,\ \zeta;\ \varsigma),\ \overline{\Upsilon}(\vartheta,\ \zeta;\ \varsigma)$ are partially real-valued differentiable functions with respect to ζ. One says

a) $\Upsilon(\vartheta,\ \zeta;)$ is $(i-g\mathcal{H})$-partially differentiable with respect to ϑ at the point $(\vartheta_0,\ \zeta_0)$, if $\partial_{\zeta(i-g\mathcal{H})}\Upsilon(\vartheta_0,\ \zeta_0;\ \varsigma) = \left[\partial_\zeta \underline{\Upsilon}(\vartheta_0,\ \zeta_0,\ \varsigma),\ \partial_\zeta \overline{\Upsilon}(\vartheta_0,\ \zeta_0;\ \varsigma)\right]$,

b) $\Upsilon(\vartheta,\ \zeta)$ is $(ii-g\mathcal{H})$-partially differentiable with respect to ϑ at the point $(\vartheta_0,\ \zeta_0)$, if $\partial_{\zeta(ii-g\mathcal{H})}\Upsilon(\vartheta_0,\ \zeta_0;\ \varsigma) = \left[\partial_\zeta \overline{\Upsilon}(\vartheta_0,\ \zeta_0,\ \varsigma),\ \partial_\zeta \underline{\Upsilon}(\vartheta_0,\ \zeta_0;\ \varsigma)\right]$.

Definition 2.6 [32] For $\rho \in [0,\ 1]$, and $Y(\zeta;\ \varsigma)$ belongs to the space of continuous fuzzy-valued functions and the space of Lebesgue-integrable fuzzy-valued functions defined on the interval $[a,\ b]$. One can express the fuzzy Caputo-FD in the $(i-g\mathcal{H})$-differentiability as follows:

$$\mathfrak{D}^{\rho}_{\zeta(i-g\mathcal{H})}\Upsilon(\zeta;\ \varsigma) = \left[\mathfrak{D}^{\rho}_{\zeta}\underline{\Upsilon}(\zeta_0,\ \varsigma),\ \mathfrak{D}^{\rho}_{\zeta}\overline{\Upsilon}(\zeta_0;\ \varsigma)\right],\ \varsigma \in [0,\ 1],$$

where

$$\mathfrak{D}^{\rho}_{\zeta}\underline{\Upsilon}(\zeta;\ \varsigma) = \frac{1}{\Gamma(m-\rho)}\left(\int_0^{\zeta}(\zeta-\tau)^{m-\rho-1}D^m_\tau\underline{\Upsilon}_{i-g\mathcal{H}}(\tau;\ \varsigma)\right)_{\zeta=\zeta_0},$$

$$\mathfrak{D}^{\rho}_{\zeta}\overline{\Upsilon}(\zeta;\ \varsigma) = \frac{1}{\Gamma(m-\rho)}\left(\int_0^{\zeta}(\zeta-\tau)^{m-\rho-1}D^m_\tau\overline{\Upsilon}_{i-g\mathcal{H}}(\tau;\ \varsigma)\right)_{\zeta=\zeta_0}.$$

Definition 2.7 [26] Let $\Upsilon(\zeta;\ \varsigma)$ be a continuous fuzzy valued function, and assume that $\Upsilon(\zeta;\ \varsigma)e^{-\omega\zeta}$, is improper fuzzy Reiman integrable on $\mathbb{R}^+$. Then, its fuzzy LT is provided as:

$$\widetilde{\mathbb{L}}\{\Upsilon(\zeta;\ \varsigma)\} = [\mathbb{L}\{\underline{\Upsilon}(\zeta;\ \varsigma)\},\ \mathbb{L}\{\overline{\Upsilon}(\zeta;\ \varsigma)\}],\ \varsigma \in [0,\ 1],$$

where

$$\mathbb{L}\{\underline{\Upsilon}(\zeta;\ \varsigma)\} = \int_0^{\infty}\underline{\Upsilon}(\zeta;\ \varsigma)e^{-\omega\zeta}d\zeta,\ \omega > 0,$$

$$\mathbb{L}\{\overline{\Upsilon}(\zeta;\ \varsigma)\} = \int_0^{\infty}\overline{\Upsilon}(\zeta;\ \varsigma)e^{-\omega\zeta}d\zeta,\ \omega > 0.$$

Theorem 2.1 [26] Let $\Upsilon(\vartheta,\ \zeta;\ \varsigma)$ belongs to the space of continuous fuzzy-valued functions and the space of Lebesgueintegrable fuzzy-valued functions defined on the interval $[a,\ b]$. Then, for $\rho \in [0,\ 1]$, the LT of fuzzy Caputo-FD in the $(i-g\mathcal{H})$-differentiability is expressed as:

$$\widetilde{\mathbb{L}}\left\{\mathfrak{D}^{\rho}_{\zeta(i-g\mathcal{H})}\gamma(\zeta;\ \varsigma)\right\} = \left[\mathbb{L}\left\{\mathfrak{D}^{\rho}_{\zeta}\underline{\Upsilon}(\zeta;\ \varsigma)\right\},\ \mathbb{L}\left\{\mathfrak{D}^{\rho}_{\zeta}\overline{\Upsilon}(\zeta;\ \varsigma)\right\}\right],\ \varsigma \in [0,\ 1],$$

where

$$\mathbb{L}\left\{\mathfrak{D}_{\zeta}^{\rho}\underline{\Upsilon}(\zeta;\ \varsigma)\right\} = \omega^{\rho}\mathbb{L}\{\underline{\Upsilon}(\zeta;\ \varsigma)\} - \omega^{\rho}\underline{\Upsilon}(0;\ \varsigma),$$

$$\mathbb{L}\left\{\mathfrak{D}_{\zeta}^{\rho}\overline{\Upsilon}(\zeta;\ \varsigma)\right\} = \omega^{\rho}\mathbb{L}\{\overline{\Upsilon}(\zeta;\ \varsigma)\} - \omega^{\rho}\overline{\Upsilon}(0;\ \varsigma).$$

3. Methodology of the proposed scheme for solving FFOPDEs

It's substantial to begin with the following theorems and some useful consequences concerning LFPSM that we will use in the current investigation.

Theorem 3.1 [31] Let the new function $\mathbb{L}\{\Upsilon(\vartheta,\ \zeta;\varsigma)\} = \Psi(\vartheta,\ \omega;\ \varsigma)$ has the following Laplace Fractional Power Series Expansion (LFPSE) :

$$\Psi(\vartheta,\ \omega;\ \varsigma) = \sum_{k=0}^{\infty} \frac{h_k(\vartheta;\ \varsigma)}{\omega^{k\rho+1}} \vartheta \in I,\ \omega > 0, \tag{1}$$

where $h_k(\vartheta;\ \varsigma) = \mathfrak{D}_{\zeta}^{m\rho}\Upsilon(\vartheta,\ 0;\ \varsigma)$.

Remark 3.1 The $\mathbb{L}^{-1}\{\Psi(\vartheta,\ \omega;\ \varsigma)\} = \Upsilon(\vartheta,\ \zeta;\ \varsigma)$, gives the following infinite generalized Taylor series form:

$$\Upsilon(\vartheta,\ \zeta;\ \varsigma) = \sum_{k=0}^{\infty} \frac{\mathfrak{D}_{\zeta}^{m\rho}\Upsilon(\vartheta,\ 0;\ \varsigma)}{\Gamma(k\rho+1)}\zeta^{\rho},\ \zeta \geq 0. \tag{2}$$

Theorem 3.2 [31]. Assume that the function $\Psi(\vartheta,\ \omega;\ \varsigma)$ can be represent as in Theorem 3.1. If $\left|\omega\mathbb{L}\left\{\mathfrak{D}_{\zeta}^{(m+1)\rho}\Upsilon(\vartheta,\ \zeta;\ \varsigma)\right\}\right| \leq \phi(\vartheta;\ \varsigma)$, then, for $0 \leq \rho \leq 1$, the remaining of the new LFPSE (1) fulfills the following inequality:

$$\Re(\vartheta,\ \zeta;\ \varsigma) \leq \frac{\phi(\vartheta;\ \varsigma)}{\omega^{(m+1)\rho+1}},\ 0 < \omega \leq \varepsilon,\ (\vartheta;\ \varsigma) \in I \times [0,\ 1]. \tag{3}$$

The semi-analytical L-FRPS scheme was created to solve both linear and nonlinear ODEs, especially those that have FDs. This technique builds a solution in the form of a fractional power series while minimizing the residual error at each iteration by combining the LT with the residual power series strategy. The LT instrument is first used to ease the processing of FDs by transforming the FODEs into an algebraic form in the Laplace domain. After that, the solution is given as a Laplace Fractional Power Series Expansion (LFPSE) series (2) with unknown coefficients that are found recursively. The inverse LT is applied to the equation as a last step, which converts the obtained expansion into a generalized Taylor series form. Because of the characteristics of the LT, the L-FRPS scheme has significant benefits like lessening the number of computations needed to generate solutions, high accuracy, quick convergence, and the capacity to naturally deal with initial conditions. The proposed method leverages the limit at infinity concept to achieve its main objective, even if it does not depend on the derivative notion for obtaining the coefficients of the series solution, like the FRPS methodology does. Additionally, the ability of the suggested approach to handle nonlinear equations is its most crucial feature. This section aims to clarify the process by which the L-FRPS scheme generates fuzzy analytical solutions to specific FFOPDEs. More particularly, we will handle in this segment the following general form of nonlinear time-FFOPDEs under Caputo-FD in the $(i - g\mathcal{H})$-differentiability by employing the L-FRPS algorithm:

$$\mathfrak{D}_{\zeta}^{\rho}\Upsilon(\vartheta,\ \zeta;\ \varsigma)=\mathcal{A}(\Upsilon,\ \Upsilon_{\vartheta},\ \Upsilon_{\vartheta\vartheta})+\mathcal{B}\left(\Upsilon,\ \Upsilon_{\vartheta},\ \Upsilon_{\vartheta\vartheta},\ \Upsilon_{\vartheta},\ \Upsilon^{2}\right), \tag{4}$$

along with the fuzzy initial condition $\Upsilon(\vartheta,\ 0;\ \varsigma)=\Lambda\varphi(\vartheta)$, for $(\vartheta,\ \zeta)\in\mathbb{R}\times[0,\ a]$, $a\in\mathbb{R}^{+}$, where $\mathfrak{D}_{\zeta}^{\rho}$ refers to fuzzy Caputo-FD in the $(i-g\mathcal{H})$-differentiability of order $\rho:0<\rho\leq 1$, $\mathcal{A},\ \mathcal{B}$ are both linear and non-linear differential operators, respectively, and Λ is a fuzzy number $\varsigma\in[0,\ 1]$.

For finding the fuzzy solution of (4), we perform the following iterations:

STEP I: Considering Eq. (4) in the parametric form as:

$$\begin{aligned}
&\mathbb{L}\left[\mathfrak{D}_{\zeta}^{\rho}\underline{\Upsilon}(\vartheta,\ \zeta;\ \varsigma)\right]=\mathbb{L}\left[\mathcal{A}(\underline{\Upsilon}\,\underline{\Upsilon}_{\vartheta},\ \underline{\Upsilon}_{\vartheta\vartheta})+\mathcal{B}(\underline{\Upsilon}\,\underline{\Upsilon}_{\vartheta},\ \underline{\Upsilon}_{\vartheta\vartheta},\ \underline{\Upsilon}\,\underline{\Upsilon}_{\vartheta},\ \underline{\Upsilon}^{2})\right],\\
&\mathbb{L}\left[\mathfrak{D}_{\zeta}^{\rho}\overline{\Upsilon}(\vartheta,\ \zeta;\ \varsigma)\right]=\mathbb{L}\left[\mathcal{A}\left(\overline{\Upsilon},\ \overline{\Upsilon}_{\vartheta},\ \overline{\Upsilon}_{\vartheta\vartheta}\right)+\mathcal{B}\left(\overline{\Upsilon},\ \overline{\Upsilon}_{\vartheta},\ \overline{\Upsilon}_{\vartheta\vartheta},\ \overline{\Upsilon}\,\overline{\Upsilon}_{\vartheta},\ \overline{\Upsilon}^{2}\right)\right].
\end{aligned} \tag{5}$$

Using the fuzzy initial condition $\Upsilon(\vartheta,\ 0;\ \varsigma)=[\underline{\Upsilon}(\vartheta,\ 0;\ \varsigma),\ \overline{\Upsilon}(\vartheta,\ 0;\ \varsigma)]=[\underline{\Lambda}(\varsigma),\ \overline{\Lambda}(\varsigma)]\varphi(\vartheta)$ and Theorem 2.1. We have the following equivalent form of Eq. (5) as:

$$\begin{aligned}
&\underline{\Psi}(\vartheta,\ \omega;\ \varsigma)=\omega^{-1}\underline{\Upsilon}(\vartheta,\ 0;\ \varsigma)+\omega^{-\rho}\mathbb{L}\left\{\mathcal{A}\mathbb{L}^{-1}\left[\underline{\Psi},\ \underline{\Psi}_{\vartheta},\ \underline{\Psi}_{\vartheta\vartheta}\right]\right\}+\omega^{-\rho}\mathbb{L}\left\{\mathcal{B}\mathbb{L}^{-1}\left[\underline{\Psi},\ \underline{\Psi}_{\vartheta},\ \underline{\Psi}_{\vartheta\vartheta},\ \underline{\Psi}\,\underline{\Psi}_{\vartheta},\ \underline{\Psi}^{2}\right]\right\},\\
&\overline{\Psi}(\vartheta,\ \omega;\ \varsigma)=\omega^{-1}\overline{\Upsilon}(\vartheta,\ 0;\ \varsigma)+\omega^{-\rho}\mathbb{L}\left\{\mathcal{A}\mathbb{L}^{-1}\left[\overline{\Psi},\ \overline{\Psi}_{\vartheta},\ \overline{\Psi}_{\vartheta\vartheta}\right]\right\}+\omega^{-\rho}\mathbb{L}\left\{\mathcal{B}\mathbb{L}^{-1}\left[\overline{\Psi},\ \overline{\Psi}_{\vartheta},\ \overline{\Psi}_{\vartheta\vartheta},\ \overline{\Psi}\,\overline{\Psi}_{\vartheta},\ \overline{\Psi}^{2}\right]\right\}.
\end{aligned} \tag{6}$$

where $\underline{\Psi}(\vartheta,\ \omega;\ \varsigma)=\widetilde{\mathbb{L}}[\underline{\Upsilon}(\vartheta,\ \zeta;\ \varsigma)]$, and $\overline{\Psi}(\vartheta,\ \omega;\ \varsigma)=\widetilde{\mathbb{L}}[\overline{\Upsilon}(\vartheta,\ \zeta;\ \varsigma)]$.

STEP II: The L-FRPS algorithm consists of representing the solutions of Eq. (6) in the following infinite LFPSEs:

$$\begin{aligned}
&\underline{\Psi}(\vartheta,\ \omega;\ \varsigma)=\sum_{k=0}^{\infty}\underline{\Lambda}(\varsigma)\frac{\gamma_k(\vartheta)}{\omega^{k\rho+1}}\vartheta\in I,\ \omega>0,\\
&\overline{\Psi}(\vartheta,\ \omega;\ \varsigma)=\sum_{k=0}^{\infty}\overline{\Lambda}(\varsigma)\frac{\delta_k(\vartheta)}{\omega^{k\rho+1}}\vartheta\in I,\ \omega>0.
\end{aligned} \tag{7}$$

Obviously, $\underline{\Lambda}(\varsigma)\gamma_0(\vartheta)=\lim_{\omega\to\infty}\omega\underline{\Psi}(\vartheta,\ \omega;\ \varsigma)=\underline{\Upsilon}(\vartheta,\ 0;\ \varsigma)=\underline{\Lambda}(\varsigma)\varphi(\vartheta)$, and $\overline{\Lambda}(\varsigma)\delta_0(\vartheta)=\lim_{\omega\to\infty}\omega\overline{\Psi}(\vartheta,\ \omega;\ \varsigma)=\overline{\Upsilon}(\vartheta,\ 0;\ \varsigma)=\overline{\Lambda}(\varsigma)\varphi(\vartheta)$. So, the infinite LFPSEs (7) will be written as:

$$\begin{aligned}
&\underline{\Psi}(\vartheta,\ \omega;\ \varsigma)=\frac{\underline{\Lambda}(\varsigma)\varphi(\vartheta)}{\omega}+\sum_{k=1}^{\infty}\underline{\Lambda}(\varsigma)\frac{\gamma_k(\vartheta)}{\omega^{k\rho+1}}\vartheta\in I,\ \omega>0,\\
&\overline{\Psi}(\vartheta,\ \omega;\ \varsigma)=\frac{\overline{\Lambda}(\varsigma)\varphi(\vartheta)}{\omega}+\sum_{k=1}^{\infty}\overline{\Lambda}(\varsigma)\frac{\delta_k(\vartheta)}{\omega^{k\rho+1}}\vartheta\in I,\ \omega>0.
\end{aligned} \tag{8}$$

Hence, the jth-LFPSEs of $\underline{\Psi}(\vartheta,\ \omega;\ \varsigma)$, and $\overline{\Psi}(\vartheta,\ \omega;\ \varsigma)$ take the forms:

$$\underline{\Psi}^j(\vartheta,\ \omega;\ \varsigma) = \frac{\underline{\Lambda}(\varsigma)\varphi(\vartheta)}{\omega} + \sum_{k=1}^{j} \underline{\Lambda}(\varsigma)\frac{\gamma_k(\vartheta)}{\omega^{k\rho+1}}\vartheta \in I,\ \omega > 0,$$

$$\overline{\Psi}^j(\vartheta,\ \omega;\ \varsigma) = \frac{\overline{\Lambda}(\varsigma)\varphi(\vartheta)}{\omega} + \sum_{k=1}^{j} \overline{\Lambda}(\varsigma)\frac{\delta_k(\vartheta)}{\omega^{k\rho+1}}\vartheta \in I,\ \omega > 0. \tag{9}$$

STEP III: The jth-Laplace Residual Error (LRE) functions of Eq. (6) may be identified as:

$$\mathbb{L}\left\{\mathrm{Res}^j\left(\underline{\Psi}^j(\vartheta,\ \omega;\ \varsigma)\right)\right\}$$

$$= \underline{\Psi}^j(\vartheta,\ \omega;\ \varsigma) - \omega^{-1}\underline{\Upsilon}(\vartheta,\ 0;\ \varsigma) - \omega^{-\rho}\mathbb{L}\left\{\mathcal{A}\mathbb{L}^{-1}\left[\underline{\Psi}^j,\ \underline{\Psi}^j_{\vartheta},\ \underline{\Psi}^j_{\vartheta\vartheta}\right]\right\}$$

$$-\omega^{-\rho}\mathbb{L}\left\{\mathcal{B}\mathbb{L}^{-1}\left[\underline{\Psi}^j,\ \underline{\Psi}^j_{\vartheta},\ \underline{\Psi}^j_{\vartheta\vartheta},\ \underline{\Psi}^j\underline{\Psi}^j_{\vartheta},\ \left(\underline{\Psi}^j\right)^2\right]\right\},$$

$$\mathbb{L}\left\{\mathrm{Res}^j\left(\overline{\Psi}^j(\vartheta,\ \omega;\ \varsigma)\right)\right\} \tag{10}$$

$$= \overline{\Psi}^j(\vartheta,\ \omega;\ \varsigma) - \omega^{-1}\overline{\Upsilon}(\vartheta,\ 0;\ \varsigma) - \omega^{-\rho}\mathbb{L}\left\{\mathcal{A}\mathbb{L}^{-1}\left[\overline{\Psi}^j,\ \overline{\Psi}^j_{\vartheta},\ \overline{\Psi}^j_{\vartheta\vartheta}\right]\right\}$$

$$-\omega^{-\rho}\mathbb{L}\left\{\mathcal{B}\mathbb{L}^{-1}\left[\overline{\Psi}^j,\ \overline{\Psi}^j_{\vartheta},\ \overline{\Psi}^j_{\vartheta\vartheta},\ \overline{\Psi}^j\overline{\Psi}^j_{\vartheta},\ \left(\overline{\Psi}^j\right)^2\right]\right\},$$

and hence the LRE functions are provided as:

$$\lim_{j\to\infty}\mathbb{L}\left\{\mathrm{Res}^j\left(\underline{\Psi}^j(\vartheta,\ \omega;\ \varsigma)\right)\right\} = \mathbb{L}\{\mathrm{Res}(\underline{\Psi}(\vartheta,\ \omega;\ \varsigma))\}$$

$$= \underline{\Psi}(\vartheta,\ \omega;\ \varsigma) - \omega^{-1}\underline{\Upsilon}(\vartheta,\ 0;\ \varsigma) - \omega^{-\rho}\mathbb{L}\left\{\mathcal{A}\mathbb{L}^{-1}\left[\underline{\Psi},\ \underline{\Psi}_{\vartheta},\ \underline{\Psi}_{\vartheta\vartheta}\right]\right\}$$

$$-\omega^{-\rho}\mathbb{L}\left\{\mathcal{B}\mathbb{L}^{-1}\left[\underline{\Psi},\ \underline{\Psi}_{\vartheta},\ \underline{\Psi}_{\vartheta\vartheta},\ \underline{\Psi}\,\underline{\Psi}_{\vartheta},\ \underline{\Psi}^2\right]\right\}$$

$$\lim_{j\to\infty}\mathbb{L}\left\{\mathrm{Res}^j\left(\overline{\Psi}^j(\vartheta,\ \omega;\ \varsigma)\right)\right\} = \mathbb{L}\{\mathrm{Res}(\overline{\Psi}(\vartheta,\ \omega;\ \varsigma))\} \tag{11}$$

$$= \overline{\Psi}_{(\vartheta,\ \omega;\ \varsigma)} - \omega^{-1}\overline{\Upsilon}(\vartheta,\ 0;\ \varsigma) - \omega^{-\rho}\mathbb{L}\left\{\mathcal{A}\mathbb{L}^{-1}\left[\overline{\Psi},\ \overline{\Psi}_{\vartheta},\ \overline{\Psi}_{\vartheta\vartheta}\right]\right\}$$

$$-\omega^{-\rho}\mathbb{L}\left\{\mathcal{B}\mathbb{L}^{-1}\left[\overline{\Psi},\ \overline{\Psi}_{\vartheta},\ \overline{\Psi}_{\vartheta\vartheta},\ \overline{\Psi}\,\overline{\Psi}_{\vartheta},\ \overline{\Psi}^2\right]\right\}.$$

STEP IV: Substitute the jth-LFPSEs of (9) into the jth-LRE of (10), and then multiply the resultant equations by the factor $\omega^{j\rho+1}$.

STEP V: The unknown coefficients $\gamma_k(\vartheta)$, and $\delta_k(\vartheta)$ for $k = 1, 2, 3, \ldots, j$ may be identified by exploring the solution of $\lim_{\omega\to\infty} \omega^{j\rho+1}\mathbb{L}\left\{\mathrm{Res}^j\left(\underline{\Psi}^j(\vartheta, \omega; \varsigma)\right)\right\} = 0$, and $\lim_{\omega\to\infty} \omega^{j\rho+1}\mathbb{L}\left\{\mathrm{Res}^j\left(\overline{\Psi}^j(\vartheta, \omega; \varsigma)\right)\right\} = 0$. This is followed by the construction of the jth-LFPSEs of (5) by aggregating the collected coefficients into it.

STEP VI: As a final step, one can implement the inverse LT operator of the acquired jth-LFPSEs in STEP V to find out the fuzzy approximate solutions of the posed model (4).

4. Applications

In many physical and biological systems, including convection, nonlinear optics, and chemical dynamics, pattern creation and front propagation are described by the well-known reaction-diffusion model known as the Newell-Whitehead-Segel (NWS) equation [37]. The model is expanded to include memory effects and uncertainties in system characteristics, which are commonly seen in complex media, through its fractional and fuzzy formulations. Whilst in compressible flow issues, such as microscale flows and porous media, where hereditary transport effects and unknown initial or boundary data are important, the fuzzy fractional gas-dynamics model is used. This model is a significant and difficult test for evaluating the stability and robustness of numerical methods since it incorporates steep gradients and nonlinear wave propagation [38]. These issues were chosen as appropriate benchmarks to show how well the suggested method handles nonlinearity, memory effects, and uncertainty propagation. This section aims to elaborate on the fuzzy approximate solutions of certain FFOPDEs along fuzzy initial data via the L-FRPS scheme involving the fuzzy Caputo-FD in the $(i-g\mathcal{H})$-differentiability operator. In addition, simulations and graphical representations of the analyzed models' outcomes were investigated. Mathematica 12 was used for both symbolic and computational tasks.

Application 4.1 Consider the fuzzy fractional gas dynamic model:

$$\begin{cases} \mathfrak{D}_{\zeta}^{\rho}\Upsilon(\vartheta,\zeta;\varsigma) - \Upsilon(\vartheta,\ \zeta;\ \varsigma) + \Upsilon(\vartheta,\ \zeta;\ \varsigma)\Upsilon_{\vartheta}(\vartheta,\ \zeta;\ \varsigma) + \Upsilon^2(\vartheta,\ \zeta;\ \varsigma) = 0,\ 0 < \rho \le 1, \\ \Upsilon(\vartheta,\ 0;\ \varsigma) = \Lambda(\varsigma)e^{-\vartheta}, \end{cases} \tag{12}$$

where $\Lambda(\varsigma) = [\underline{\Lambda}(\varsigma),\ \overline{\Lambda}(\varsigma)] = [\varsigma,\ 3-2\varsigma],\ \varsigma \in [0,\ 1]$ is a fuzzy number.

Based on the prior discussion in Section 3, we have the following parameterized formulation of the fuzzy fractional gas dynamic model (12):

$$\begin{cases} \mathfrak{D}_{\zeta}^{\rho}\underline{\Upsilon}(\vartheta,\ \zeta;\ \varsigma) - \underline{\Upsilon}(\vartheta,\ \zeta;\ \varsigma) + \underline{\Upsilon}(\vartheta,\ \zeta;\ \varsigma)\underline{\Upsilon}_{\vartheta}(\vartheta,\ \zeta;\ \varsigma) + \underline{\Upsilon}^2(\vartheta,\ \zeta;\ \varsigma) = 0, \\ \underline{\Upsilon}(\vartheta,\ 0;\ \varsigma) = \varsigma e^{-\vartheta}, \\ \mathfrak{D}_{\zeta}^{\rho}\overline{\Upsilon}(\vartheta,\ \zeta;\ \varsigma) - \overline{\Upsilon}(\vartheta,\ \zeta,\ \varsigma) + \overline{\Upsilon}(\vartheta,\ \zeta;\ \varsigma)\Upsilon_{\vartheta}(\vartheta,\ \zeta;\ \varsigma) + \overline{\Upsilon}^2(\vartheta,\ \zeta;\ \varsigma) = 0, \\ \overline{\Upsilon}(\vartheta,\ 0;\ \varsigma) = (3-2\varsigma)e^{-\vartheta}. \end{cases} \tag{13}$$

Running the LT of (13) and using their initial conditions yields:

$$\begin{aligned}
&\underline{\Psi}(\vartheta,\ \omega;\ \varsigma)-\varsigma e^{-\vartheta}\omega^{-1}-\omega^{-\rho}\underline{\Psi}(\vartheta,\ \omega;\ \varsigma)+\omega^{-\rho}\mathbb{L}\left\{\mathbb{L}^{-1}\left[\underline{\Psi}(\vartheta,\ \omega;\ \varsigma)\underline{\Psi}_{\vartheta}(\vartheta,\ \omega;\ \varsigma)\right]\right\}\\
&+\omega^{-\rho}\mathbb{L}\left\{\mathbb{L}^{-1}\left[\underline{\Psi}^{2}(\vartheta,\ \omega;\ \varsigma)\right]\right\}=0,\\
&\overline{\Psi}(\vartheta,\ \omega;\ \varsigma)-(3-2\varsigma)e^{-\vartheta}\omega^{-1}-\omega^{-\rho}\overline{\Psi}(\vartheta,\ \omega;\ \varsigma)+\omega^{-\rho}\mathbb{L}\left\{\mathbb{L}^{-1}\left[\overline{\Psi}(\vartheta,\ \omega;\ \varsigma)\overline{\Psi}_{\vartheta}(\vartheta,\ \omega;\ \varsigma)\right]\right\}\\
&+\omega^{-\rho}\mathbb{L}\left\{\mathbb{L}^{-1}\left[\overline{\Psi}^{2}(\vartheta,\ \omega;\ \varsigma)\right]\right\}=0.
\end{aligned}\tag{14}$$

To explore the approximate solutions to the posed problem, we should first determine the form of the unknown functions $\gamma_n(\vartheta)$, and $\delta_n(\vartheta)$ for $n = 1,\ 2,\ \ldots,\ j$. To accomplish this, we use the j-th transform functions $\underline{\Psi}^j(\vartheta,\ \omega;\ \varsigma)$, and $\overline{\Psi}^j(\vartheta,\ \omega;\ \varsigma)(10)$ into the jth-LRE (11), and then by solving the system $\lim_{\omega\to\infty}\omega^{j\rho+1}\mathbb{L}\left\{\mathrm{Res}^j\left(\underline{\Psi}^j(\vartheta,\ \omega;\ \varsigma)\right)\right\}=0$, and $\lim_{\omega\to\infty}\omega^{j\rho+1}\mathbb{L}\left\{\mathrm{Res}^j\left(\overline{\Psi}^j(\vartheta,\ \omega;\ \varsigma)\right)\right\}=0$, we have the following

$$\begin{aligned}
\gamma_j(\vartheta;\ \varsigma)&=\varsigma\left(\gamma_{j-1}(\vartheta)-\Gamma((j-1)\rho+1)\sum_{i=0}^{j-1}\frac{\gamma_i(\vartheta)\gamma'_{j-i-1}(\vartheta)}{\Gamma(i\rho+1)\Gamma((j-i-1)\rho+1)}\right.\\
&\left.-\Gamma((j-1)\rho+1)\sum_{i=0}^{j-1}\frac{\gamma_i(\vartheta)\gamma_{j-i-1}(\vartheta)}{\Gamma(i\rho+1)\Gamma((j-i-1)\rho+1)}\right),\\
\delta_j(\vartheta;\ \varsigma)&=(3-2\varsigma)\left(\delta_{j-1}(\vartheta)-\Gamma((j-1)\rho+1)\sum_{i=0}^{j-1}\frac{\delta_i(\vartheta)\delta'_{j-i-1}(\vartheta)}{\Gamma(i\rho+1)\Gamma((j-i-1)\rho+1)}\right.\\
&\left.-\Gamma((j-1)\rho+1)\sum_{i=0}^{j-1}\frac{\delta_i(\vartheta)\delta_{j-i-1}(\vartheta)}{\Gamma(i\rho+1)\Gamma((j-i-1)\rho+1)}\right).
\end{aligned}\tag{15}$$

Considering the initial unknown functions $\gamma_0(\vartheta)=e^{-\vartheta}$, and $\delta_0(\vartheta)=e^{-\vartheta}$, and utilizing the Mathematica Software 12, we can immediately discover the parameters required $\gamma_j(\vartheta;\ \varsigma)=\varsigma e^{-\vartheta}$, and $\delta_j(\vartheta;\ \varsigma)=(3-2\varsigma)e^{-\vartheta}$ for $j=1,\ 2,\ 3,\ \ldots$. By combining the results gained with expansions (10), we may anticipate the j-th LFPSEs of (13) as follows:

$$\begin{aligned}
\underline{\Psi}^j(\vartheta,\ \omega;\ \varsigma)&=\varsigma\left(\frac{e^{-\vartheta}}{\omega}+\sum_{k=1}^{j}\frac{e^{-\vartheta}}{\omega^{k\rho+1}}\right),\\
\overline{\Psi}^j(\vartheta,\ \omega;\ \varsigma)&=(3-2\varsigma)\left(\frac{e^{-\vartheta}}{\omega}+\sum_{k=1}^{j}\frac{e^{-\vartheta}}{\omega^{k\rho+1}}\right).
\end{aligned}\tag{16}$$

When $j\to\infty$, the LFPSEs of (14) have the following infinite series forms:

$$
\underline{\Psi}^j(\vartheta,\ \omega;\ \varsigma) = \varsigma\left(\frac{e^{-\vartheta}}{\omega} + \sum_{k=1}^{\infty}\frac{e^{-\vartheta}}{\omega^{k\rho+1}}\right) = \varsigma e^{-\vartheta}\sum_{k=0}^{\infty}\frac{1}{\omega^{k\rho+1}},
$$

$$
\overline{\Psi}^j(\vartheta,\ \omega;\ \varsigma) = (3-2\varsigma)\left(\frac{e^{-\vartheta}}{\omega} + \sum_{k=1}^{\infty}\frac{e^{-\vartheta}}{\omega^{k\rho+1}}\right) = (3-2\varsigma)\sum_{k=0}^{\infty}\frac{e^{-\vartheta}}{\omega^{k\rho+1}}. \tag{17}
$$

By taking Inverse LT to (17), the approximate solutions of (13) could be expressed as the closed forms listed below:

$$
\underline{\Upsilon}(\vartheta,\ \zeta;\varsigma) = \varsigma e^{-\vartheta}\sum_{k=0}^{\infty}\frac{\zeta^{\rho}}{\Gamma(k\rho+1)} = \varsigma e^{-\vartheta}E_{\rho}\left(\zeta^{\rho}\right),
$$

$$
\overline{\Upsilon}(\vartheta,\ \zeta;\ \varsigma) = (3-2\varsigma)e^{-\vartheta}\sum_{k=0}^{\infty}\frac{\zeta^{\rho}}{\Gamma(k\rho+1)} = (3-2\varsigma)E_{\rho}\left(\zeta^{\rho}\right), \tag{18}
$$

which is compatible with the analytical findings that FADM derived [28]. So, that for $\rho = 1$, the exact solution of the fuzzy fractional gas dynamic model has the general form: $\Upsilon(\vartheta,\ \zeta;\ \varsigma) = [\varsigma,\ 3-2\varsigma]e^{\zeta-\vartheta}$.

Table 1. Absolute errors of the approximating $\underline{\Upsilon}_6(\vartheta,\ \zeta;\ \varsigma)$ for Application 4.1

ϑ	ζ	$\varsigma = 0.25$	$\varsigma = 0.5$	$\varsigma = 0.75$	$\varsigma = 1$
	0.1	1.008909×10^{-10}	2.017817×10^{-10}	3.026698×10^{-10}	4.035634×10^{-10}
	0.3	2.263439×10^{-7}	4.526879×10^{-7}	6.790318×10^{-7}	9.053757×10^{-7}
-3	0.5	8.298563×10^{-6}	1.659712×10^{-5}	2.489569×10^{-5}	3.319425×10^{-5}
	0.7	8.982963×10^{-5}	1.796592×10^{-4}	2.694888×10^{-4}	3.593185×10^{-4}
	0.9	5.360260×10^{-4}	1.072052×10^{-3}	1.608078×10^{-3}	2.144104×10^{-3}
	0.1	3.384424×10^{-14}	6.768848×10^{-14}	1.015324×10^{-13}	1.353769×10^{-13}
	0.3	7.592992×10^{-11}	1.518599×10^{-10}	2.277897×10^{-10}	3.037197×10^{-10}
5	0.5	2.783857×10^{-9}	5.567716×10^{-9}	8.351566×10^{-9}	1.113543×10^{-8}
	0.7	3.013448×10^{-8}	6.026896×10^{-8}	9.040345×10^{-8}	1.205379×10^{-7}
	0.9	1.798167×10^{-7}	3.596334×10^{-7}	5.394501×10^{-7}	7.192667×10^{-7}

Table 1 provides the absolute errors of numerically approximating the lower exact solution by $\underline{\Upsilon}_6(\vartheta,\ \zeta;\ \varsigma)$, for different uncertainty ς-levels such as $\varsigma \in \{0.25,\ 0.5,\ 0.75,\ 1\}$ at $\rho = 1$, with fixed values ϑ. The table demonstrates that bigger ζ values widen the fuzzy solution band, while absolute errors stay very tiny (down to 10^{-12}) and decrease as $\rho \to 1$. Also, listed below are some graphical representations of gas fractional Initial Value Problems (IVPs) (12) produced using the algorithm discussed, shown in Figures 1, 2, and 3. Including the lower and upper plots of exact and the sixth-truncation approximate solutions of Application 4.1 for a variety of ς-level and the parameter ρ as shown in Figure 1a and b over a sufficiently temporal domain and a fixed value of ϑ. Further, Figures 2 and 3 show the 2D- and 3D-simulation of the exact and the sixth-truncation approximate solutions of lower and upper fuzzy levels with a diversity of ρ over $\varsigma \in [0,\ 1]$. These figures demonstrate that, for a fixed value of ρ, the approximate solutions obtained using the suggested method for the chosen grid points are legitimate and in good agreement with one another, close to the exact solutions, and confirm the efficiency and accuracy of our algorithm in Application 4.1, while increasing values of uncertainty ς-levels enlarge the fuzzy solution band. These findings demonstrate that when the uncertainty ς-levels or/and Caputo-FD parameters vary, there is good agreement between the solutions. Furthermore, these figures demonstrate that the outcomes meet the convex symmetry.

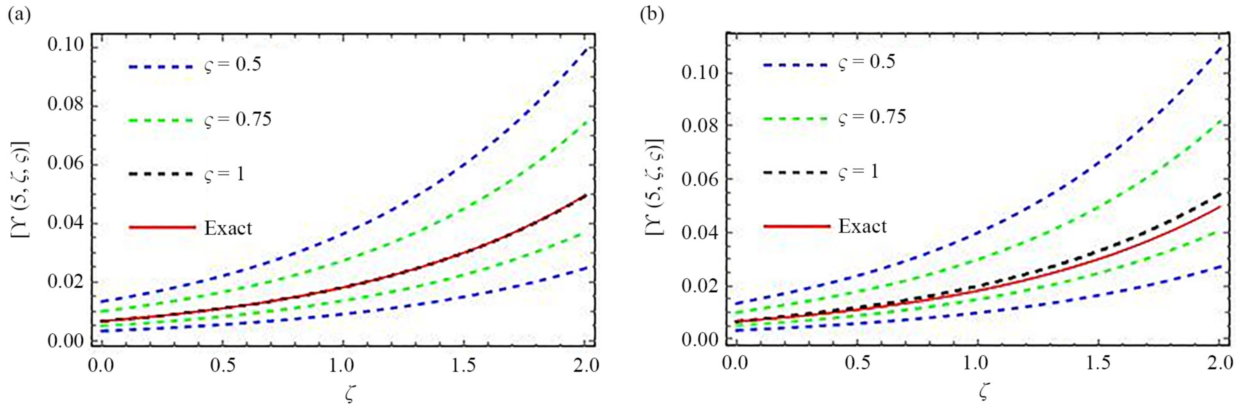

Figure 1. Plots of fuzzy lower and upper portions for Application 4.1; (a) $[\Upsilon(\vartheta,\ \zeta;\ \varsigma)]$, and $[\Upsilon_6(\vartheta,\ \zeta;\ \varsigma)]$ at $\rho = 1$; $(b)[\Upsilon(\vartheta,\ \zeta;\ \varsigma)]$, and $[\Upsilon_6(\vartheta,\ \zeta;\ \varsigma)]$ at $\rho = 0.9$

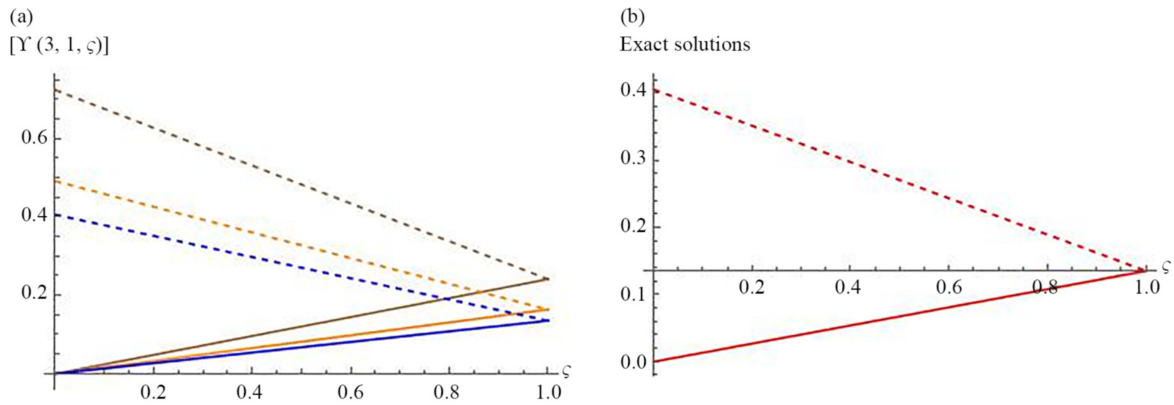

Figure 2. Plots of triangle fuzzy solutions at fixed values $\vartheta = 3$, and $\zeta = 1$; (a) $[\Upsilon_6(\vartheta,\ \zeta;\ \varsigma)]$; $\rho \in \{0.5,\ 0.8,\ 1\}$; (b) Exact solutions

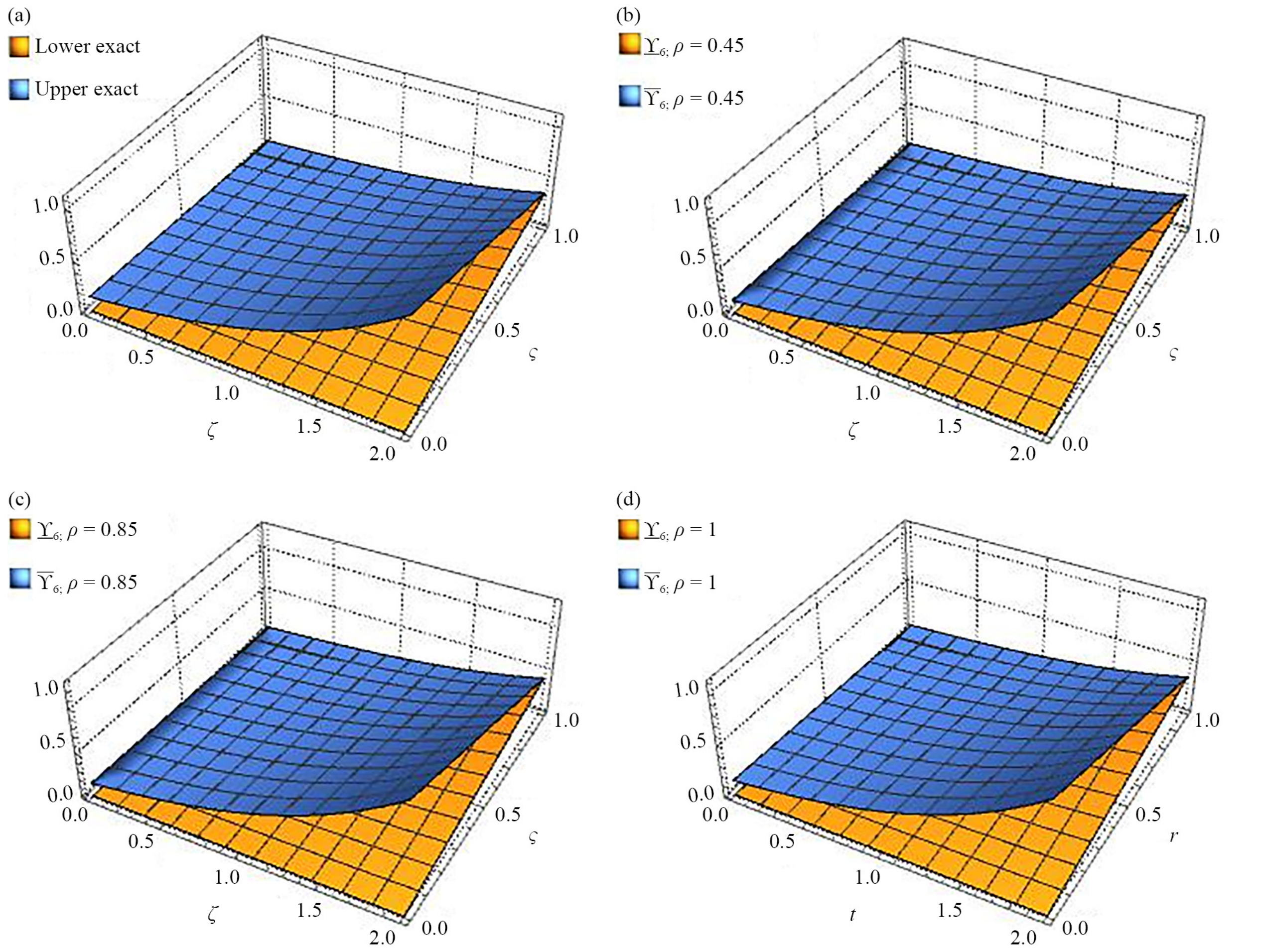

Figure 3. Surface behavior of findings for Application 4.1; (a) Fuzzy lower and upper exact solutions; (b) $\underline{\Upsilon}_6(\vartheta,\ \zeta;\ \varsigma)$, and $\overline{\Upsilon}_6(\vartheta,\ \zeta;\ \varsigma)$ when $\rho = 0.45$; (c) $\underline{\Upsilon}_6(\vartheta,\ \zeta;\varsigma)$, and $\overline{\Upsilon}_6(\vartheta,\ \zeta;\ \varsigma)$ when $\rho = 0.85$; (d) $\underline{\Upsilon}_6(\vartheta,\ \zeta;\ \varsigma)$, and $\overline{\Upsilon}_6(\vartheta,\ \zeta;\ \varsigma)$ when $\rho = 1$

Application 4.2 Consider the fuzzy fractional advection model:

$$\begin{cases} \mathfrak{D}_{\zeta}^{\rho}\Upsilon(\vartheta,\ \zeta;\ \varsigma) + \Upsilon(\vartheta,\ \zeta;\varsigma)\Upsilon_{\vartheta}(\vartheta,\ \zeta;\ \varsigma) = 0,\ 0 < \rho \leq 1, \\ \\ \Upsilon(\vartheta,\ 0;\ \varsigma) = -\Lambda(\varsigma)\vartheta, \end{cases} \tag{19}$$

where $\Lambda(\varsigma) = [\underline{\Lambda}(\varsigma),\ \overline{\Lambda}(\varsigma)] = [\varsigma - 1,\ 1 - \varsigma],\ \varsigma \in [0,\ 1]$ is a fuzzy number.

The parametric form of (19) is shown as:

$$\begin{cases} \mathfrak{D}_{\zeta}^{\rho}\underline{\Upsilon}(\vartheta,\ \zeta;\ \varsigma)+\underline{\Upsilon}(\vartheta,\ \zeta;\ \varsigma)\underline{\Upsilon}_{\vartheta}(\vartheta,\ \zeta;\ \varsigma)=0, \\ \underline{\Upsilon}(\vartheta,\ 0;\ \varsigma)=-(\varsigma-1)\vartheta, \\ \mathfrak{D}_{\zeta}^{\rho}\overline{\Upsilon}(\vartheta,\ \zeta;\ \varsigma)+\overline{\Upsilon}(\vartheta,\ \zeta;\ \varsigma)\Upsilon_{\vartheta}(\vartheta,\ \zeta;\ \varsigma)=0, \\ \overline{\Upsilon}(\vartheta,\ 0;\ \varsigma)=-(1-\varsigma)\vartheta. \end{cases} \tag{20}$$

After taking the LT into the lower and upper parts of the fuzzy fractional advection model (20), and considering their ICs, we obtain

$$\begin{aligned} &\underline{\Psi}(\vartheta,\ \omega;\ \varsigma)+(\varsigma-1)\vartheta\omega^{-1}+\omega^{-\rho}\mathbb{L}\left\{\mathbb{L}^{-1}\left[\underline{\Psi}(\vartheta,\ \omega;\ \varsigma)\underline{\Psi}_{\vartheta}(\vartheta,\ \omega;\ \varsigma)\right]\right\}=0, \\ &\overline{\Psi}(\vartheta,\ \omega;\ \varsigma)+(1-\varsigma)\vartheta\omega^{-1}+\omega^{-\rho}\mathbb{L}\left\{\mathbb{L}^{-1}\left[\overline{\Psi}(\vartheta,\ \omega;\ \varsigma)\overline{\Psi}_{\vartheta}(\vartheta,\ \omega;\ \varsigma)\right]\right\}=0. \end{aligned} \tag{21}$$

Referring to the previously indicated approach arguments, the j-th LFPSEs $\underline{\Psi}^{j}(\vartheta,\ \omega;\ \varsigma)$, and $\overline{\Psi}^{j}(\vartheta,\ \omega;\ \varsigma)$ of (21) are expressed as:

$$\begin{aligned} &\underline{\Psi}^{j}(\vartheta,\ \omega;\ \varsigma)=-\frac{(\varsigma-1)\vartheta}{\omega}+\sum_{k=1}^{j}\underline{\Lambda}(\varsigma)\frac{\gamma_k(\vartheta)}{\omega^{k\rho+1}}\vartheta\in I,\ \omega>0, \\ &\overline{\Psi}^{j}(\vartheta,\ \omega;\ \varsigma)=-\frac{(1-\varsigma)\vartheta}{\omega}+\sum_{k=1}^{j}\overline{\Lambda}(\varsigma)\frac{\delta_k(\vartheta)}{\omega^{k\rho+1}}\vartheta\in I,\ \omega>0, \end{aligned} \tag{22}$$

and hence the j th-LRE of (21) will be defined as:

$$\begin{aligned} \mathbb{L}\left\{\mathrm{Res}^{j}\left(\underline{\Psi}^{j}(\vartheta,\ \omega;\ \varsigma)\right)\right\}=&\sum_{k=1}^{j}\underline{\Lambda}(\varsigma)\frac{\gamma_k(\vartheta)}{\omega^{k\rho+1}}+\omega^{-\rho}\mathbb{L} \\ &\left\{\mathbb{L}^{-1}\left[\left(\frac{\underline{\Lambda}(\varsigma)\varphi(\vartheta)}{\omega}+\sum_{k=1}^{j}\underline{\Lambda}(\varsigma)\frac{\gamma_k(\vartheta)}{\omega^{k\rho+1}}\right)\left(\frac{\underline{\Lambda}(\varsigma)\varphi'(\vartheta)}{\omega}+\sum_{k=1}^{j}\underline{\Lambda}(\varsigma)\frac{\gamma_k'(\vartheta)}{\omega^{k\rho+1}}\right)\right]\right\}, \\ \mathbb{L}\left\{\mathrm{Res}^{j}\left(\overline{\Psi}^{j}(\vartheta,\ \omega;\ \varsigma)\right)\right\}=&\sum_{k=1}^{j}\overline{\Lambda}(\varsigma)\frac{\delta_k(\vartheta)}{\omega^{k\rho+1}}+\omega^{-\rho}\mathbb{L} \\ &\left\{\mathbb{L}^{-1}\left[\left(\frac{\overline{\Lambda}(\varsigma)\varphi(\vartheta)}{\omega}+\sum_{k=1}^{j}\overline{\Lambda}(\varsigma)\frac{\delta_k(\vartheta)}{\omega^{k\rho+1}}\right)\left(\frac{\overline{\Lambda}(\varsigma)\varphi'(\vartheta)}{\omega}+\sum_{k=1}^{j}\overline{\Lambda}(\varsigma)\frac{\delta_k'(\vartheta)}{\omega^{k\rho+1}}\right)\right]\right\}. \end{aligned} \tag{23}$$

Then, by solving the system $\lim_{\omega\to\infty} \omega^{j\rho+1}\mathbb{L}\left\{\mathrm{Res}^j\left(\underline{\Psi}^j(\vartheta,\ \omega;\ \varsigma)\right)\right\}=0$, and $\lim_{\omega\to\infty} \omega^{j\rho+1}\mathbb{L}\left\{\mathrm{Res}^j\left(\overline{\Psi}^j(\vartheta,\ \omega;\ \varsigma)\right)\right\}=0$, we have the following recursive formula:

$$\begin{aligned}
\gamma_j(\vartheta;\ \varsigma) &= (\varsigma-1)\left(-\Gamma((j-1)\rho+1)\sum_{i=0}^{j-1}\frac{\gamma_i(\vartheta)\gamma'_{j-i-1}(\vartheta)}{\Gamma(i\rho+1)\Gamma((j-i-1)\rho+1)}\right),\\
\delta_j(\vartheta;\ \varsigma) &= (1-\varsigma)\left(-\Gamma((j-1)\rho+1)\sum_{i=0}^{j-1}\frac{\delta_i(\vartheta)\delta'_{j-i-1}(\vartheta)}{\Gamma(i\rho+1)\Gamma((j-i-1)\rho+1)}\right).
\end{aligned} \tag{24}$$

Using the MATHEMATICA Software Package 12 and the obtained recurrence relation (24), we determined the following first four unknown functions of the LFPSEs of (22), considering $\gamma_0(\vartheta)=\delta_0(\vartheta)=-\vartheta$:

$$\gamma_1(\vartheta;\ \varsigma)=-(\varsigma-1)^2\vartheta,$$

$$\gamma_2(\vartheta;\ \varsigma)=-2(\varsigma-1)^3\vartheta,$$

$$\gamma_3(\vartheta;\ \varsigma)=-\left(\frac{(\varsigma-1)^4\vartheta\left(4\Gamma(\rho+1)^2+\Gamma(2\rho+1)\right)}{\Gamma(\rho+1)^2}\right),$$

$$\gamma_4(\vartheta;\ \varsigma)=-2(\varsigma-1)^5\vartheta\left(4+\frac{\Gamma(2\rho+1)}{\Gamma^2(\rho+1)}+\frac{2\Gamma(3\rho+1)}{\Gamma(\rho+1)\Gamma(2\rho+1)}\right).$$

and

$$\delta_1(\vartheta;\ \varsigma)=-(1-\varsigma)^2\vartheta,$$

$$\delta_2(\vartheta;\ \varsigma)=-2(1-\varsigma)^3\vartheta,$$

$$\delta_3(\vartheta;\ \varsigma)=-\left(\frac{(\varsigma-1)^4\vartheta\left(4\Gamma(\rho+1)^2+\Gamma(2\rho+1)\right)}{\Gamma(\rho+1)^2}\right),$$

$$\delta_4(\vartheta;\ \varsigma)=2(\varsigma-1)^5\vartheta\left(\frac{\dfrac{4^\alpha\Gamma\left(\rho+\frac{1}{2}\right)}{\sqrt{\pi}}+\dfrac{2\Gamma(3\rho+1)}{\Gamma(2\rho+1)}}{\Gamma(\rho+1)}+4\right).$$

Furthermore, the components $\gamma_j(\vartheta;\ \varsigma)$, and $\delta_j(\vartheta;\ \varsigma)$ for each $j\geq 5$ can be listed similarly. The gained j terms in the shape of an infinite series are then used to create the approximate solutions $\underline{\Psi}(\vartheta,\ \omega;\ \varsigma)$, $\overline{\Psi}(\vartheta,\ \omega;\ \varsigma)$ as follows:

$$
\begin{cases}
\underline{\Psi}(\vartheta,\ \omega;\ \varsigma) = \dfrac{1-\varsigma}{\omega} - \dfrac{(\varsigma-1)\vartheta}{\omega^{\rho+1}} - \dfrac{(\varsigma-1)^2\vartheta}{\omega^{2\rho+1}} - \dfrac{2(\varsigma-1)^3\vartheta}{\omega^{3\rho+1}} \\
\qquad - \left(\dfrac{(\varsigma-1)^4\vartheta\left(4\Gamma(\rho+1)^2+\Gamma(2\rho+1)\right)}{\Gamma(\rho+1)^2}\right)\dfrac{1}{\omega^{4\rho+1}} + \ldots, \\
\overline{\Psi}(\vartheta,\ \omega;\ \varsigma) = \dfrac{\varsigma-1}{\omega} - \dfrac{(1-\varsigma)\vartheta}{\omega^{\rho+1}} - \dfrac{(1-\varsigma)^2\vartheta}{\omega^{\rho+1}} - \dfrac{2(1-\varsigma)^3\vartheta}{\omega^{3\rho+1}} \\
\qquad - \left(\dfrac{(\varsigma-1)^4\vartheta\left(4\Gamma(\rho+1)^2+\Gamma(2\rho+1)\right)}{\Gamma(\rho+1)^2}\right)\dfrac{1}{\omega^{4\rho+1}} + \ldots.
\end{cases} \tag{25}
$$

Finally, apply the inverse LT to both sides of (25) to obtain the LFPSEs $\underline{\Upsilon}(\vartheta,\ \zeta;\ \varsigma)$, and $\overline{\Upsilon}(\vartheta,\ \zeta;\ \varsigma)$ for the parametrized equation (20):

$$
\begin{aligned}
\underline{\Upsilon}(\vartheta,\ \zeta;\ \varsigma) &= \vartheta\left(1-\varsigma-\frac{(\varsigma-1)^2\zeta^{\rho}}{\Gamma(\rho+1)} - \frac{2(\varsigma-1)^3\zeta^{2\rho}}{\Gamma(2\rho+1)} - \frac{(\varsigma-1)^4\zeta^{3\rho}\left(4\Gamma(\rho+1)^2+\Gamma(2\rho+1)\right)}{\Gamma(\rho+1)^2\Gamma(3\rho+1)}\right)+\ldots, \\
\overline{\Upsilon}(\vartheta,\ \zeta;\ \varsigma) &= \vartheta\left(\varsigma-1-\frac{(1-\varsigma)^2\zeta^{\rho}}{\Gamma(\rho+1)} - \frac{2(1-\varsigma)^3\zeta^{2\rho}}{\Gamma(2\rho+1)} - \frac{(1-\varsigma)^4\zeta^{3\rho}\left(4\Gamma(\rho+1)^2+\Gamma(2\rho+1)\right)}{\Gamma(\rho+1)^2\Gamma(3\rho+1)}\right)+\ldots.
\end{aligned} \tag{26}
$$

As a result, the approximate solutions of (20) at $\rho = 1$ can be expressed as:

$$
\begin{aligned}
\underline{\Upsilon}(\vartheta,\ \zeta;\ \varsigma) &= \vartheta\left(1-\varsigma-(\varsigma-1)^2\zeta-(\varsigma-1)^3\zeta^2-(\varsigma-1)^4\zeta^3\right)+\ldots, \\
\overline{\Upsilon}(\vartheta,\ \zeta;\ \varsigma) &= \vartheta\left(\varsigma-1-(1-\varsigma)^2\zeta-(1-\varsigma)^3\zeta^2-(1-\varsigma)^4\zeta^3\right)+\ldots,
\end{aligned} \tag{27}
$$

which are completely in harmony with the Taylor series of the exact solutions $\underline{\Upsilon}(\vartheta,\ \zeta;\ \varsigma) = \dfrac{(\varsigma-1)\vartheta}{(\varsigma-1)\zeta-1}$, and $\overline{\Upsilon}(\vartheta,\ \zeta;\ \varsigma) = \dfrac{(1-\varsigma)\vartheta}{(1-\varsigma)\zeta-1}$, as met acquired results by ADM [28].

To demonstrate the accuracy and effectiveness of the suggested approach, the absolute errors of numerically approximating $[\Upsilon(0.5,\ \zeta;\ 0.8)]$ by $[\Upsilon_6(0.5,\ \zeta;\ 0.8)]$ have been computed and listed in Table 2 at a fixed uncertain level and distinct values of fractional order. Additionally, the numerical outcomes of the sixth approximate solutions for Application 4.2 at various values of fractional order ρ, with certain chosen grid points provided in Table 3. The findings tabulated validate the stability of the LFRPS approach by showing that an increase ρ produces solutions that more closely resemble the classical (integer-order) case. In the following 2D graphical simulations of the fuzzy exact and sixth approximate solutions for the model studied (19), as illustrated in Figure 4. In Figure 5, the 3D surface behavior of the findings by the L-FRPS algorithm for the fractional IVP system (20) is depicted. These analysis data demonstrate the superiority of the L-FRPS approach, and the outcomes demonstrate how the solution surface transitions smoothly with memory effects and how reliable the L-FRPS Method (LFRPSM) is in a context of uncertainty. Furthermore, the absolute errors were computed for Application 4.2 utilizing the LFRPSM with the ADM [28] for a fixed value of ς and various values of ζ for the sake of numerical comparisons, as indicated in Table 4. This table makes it evident that, in terms of accuracy and applicability, our approach is superior to the previously discussed method.

Table 2. Absolute errors of the approximating $[\Upsilon_6(0.5,\ \zeta;\ 0.8)]$ for Application 4.2

ζ	$\rho = 1$	$\rho = 0.95$	$\rho = 0.85$
0.18	$[7.56413, 8.12908]\times 10^{-12}$	$[3.66388, 4.44217]\times 10^{-4}$	$[3.66388, 4.44217]\times 10^{-4}$
0.36	$[9.35692, 10.0809]\times 10^{-10}$	$[4.35699, 6.5885]\times 10^{-4}$	$[4.35699, 6.5885]\times 10^{-4}$
0.54	$[1.54677, 1.92133]\times 10^{-8}$	$[4.07489, 8.02802]\times 10^{-4}$	$[4.07489, 8.02802]\times 10^{-4}$
0.72	$[1.12231, 1.4999]\times 10^{-7}$	$[3.26577, 9.03295]\times 10^{-4}$	$[3.26577, 9.03295]\times 10^{-4}$
0.9	$[5.18831, 7.4661]\times 10^{-7}$	$[2.14131, 9.71016]\times 10^{-4}$	$[2.14131, 9.71016]\times 10^{-4}$

Table 3. Numerical findings of the approximating $[\underline{\Upsilon}_6(1,\ \zeta;\ \varsigma)]$ for Application 4.2

ζ	$\varsigma = 0.5$		
	$\rho = 1$	$\rho = 0.9$	$\rho = 0.7$
0.25	$[0.444445, -0.571428]$	$[0.435887, -0.589427]$	$[0.418156, -0.645294]$
0.5	$[0.400024, -0.666626]$	$[0.393438, -0.701527]$	$[0.383903, -0.813632]$
0.75	$[0.364016, -0.799166]$	$[0.361853, -0.859907]$	$[0.367720, -1.062997]$
1	$[0.335938, -0.992188]$	$[0.341057, -1.095899]$	$[0.376465, -1.443059]$
	$\varsigma = 0.75$		
0.25	$[0.235294, -0.266667]$	$[0.232756, -0.270340]$	$[0.227086, -0.280304]$
0.5	$[0.222222, -0.285714]$	$[0.219805, -0.291172]$	$[0.215366, -0.304894]$
0.75	$[0.210528, -0.307691]$	$[0.208910, -0.314499]$	$[0.206593, -0.330925]$
1	$[0.200012, -0.333313]$	$[0.199481, -0.341288]$	$[0.199563, -0.359876]$

Table 4. Comparison of numerical absolute errors for Application 4.2

ζ	$\varsigma = 0.4$		$\varsigma = 0.8$	
	L-FRPSM	ADM [28]	L-FRPSM	ADM [28]
0.18	$[3.978, 4.941]\times 10^{-6}$	$[3.683, 4.575]\times 10^{-5}$	$[5.836, 6.272]\times 10^{-9}$	$[1.621, 1.742]\times 10^{-7}$
0.36	$[1.160, 1.799]\times 10^{-4}$	$[5.370, 8.329]\times 10^{-4}$	$[1.804, 2.085]\times 10^{-7}$	$[2.506, 2.895]\times 10^{-6}$
0.54	$[8.090, 1.584]\times 10^{-4}$	$[2.496, 4.890]\times 10^{-3}$	$[1.326, 1.647]\times 10^{-6}$	$[1.227, 1.525]\times 10^{-5}$
0.72	$[3.152, 7.946]\times 10^{-3}$	$[7.296, 0.183]\times 10^{-2}$	$[5.412, 7.233]\times 10^{-6}$	$[3.758, 5.023]\times 10^{-5}$
0.9	$[0.894, 2.994]\times 10^{-2}$	$[1.656, 5.545]\times 10^{-2}$	$[1.601, 2.304]\times 10^{-5}$	$[8.896, 0.1280]\times 10^{-5}$

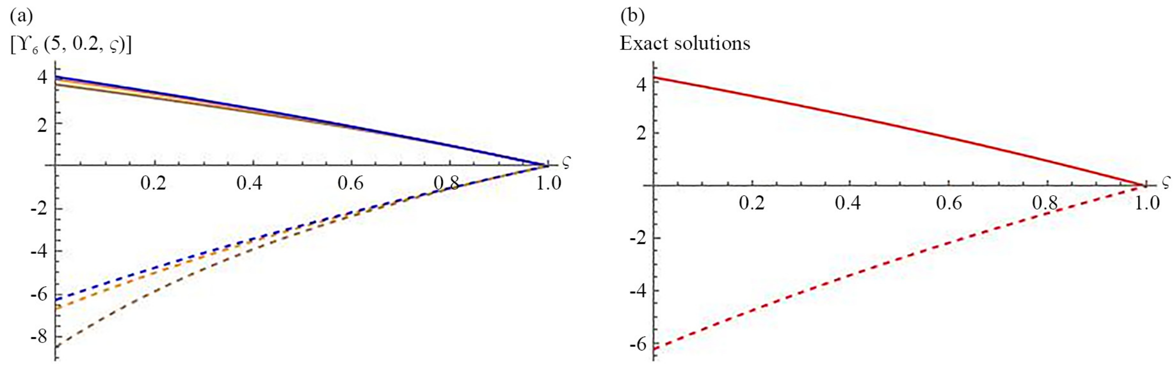

Figure 4. Plots of triangle fuzzy solutions at fixed values $\vartheta = 5$, and $\zeta = 0.2$; (a) $[\Upsilon_6(\vartheta,\ \zeta;\ \varsigma)]$; $\rho \in \{0.5,\ 0.8,\ 1\}$; (b) Exact solutions

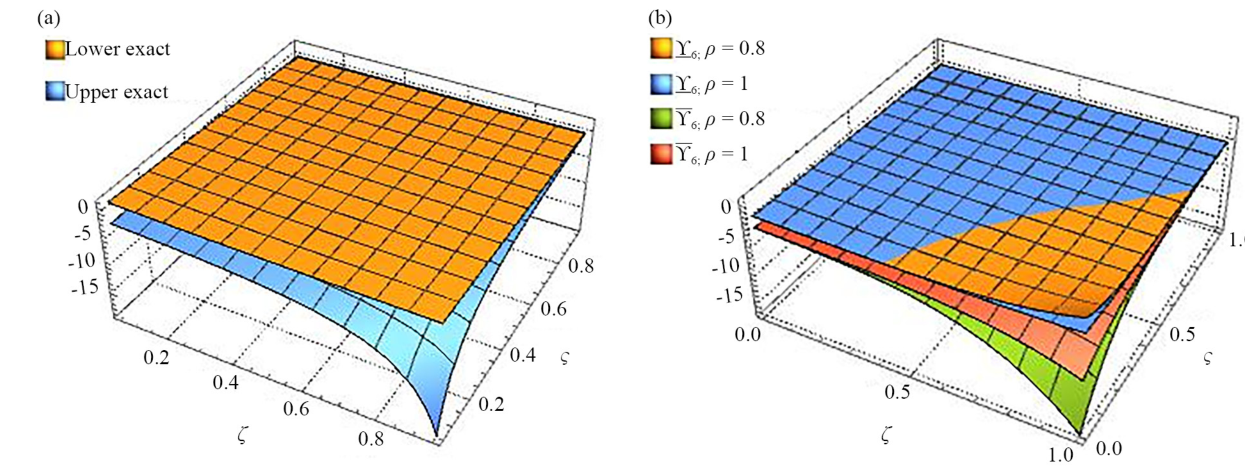

Figure 5. Surface behavior of findings for Application 4.2; (a) Fuzzy lower and upper exact solutions; (b) $\underline{\Upsilon}_6(1,\ \zeta;\ \varsigma)$, and $\overline{\Upsilon}_6(1,\ \zeta;\ \varsigma)$ when $\rho = 0.8$, and $\rho = 1$

Application 4.3 Consider the fuzzy fractional Newell-Whitehead-Segel model:

$$\begin{cases} \mathfrak{D}_{\zeta}^{\rho}\Upsilon(\vartheta,\ \zeta;\ \varsigma) - \Upsilon_{\vartheta\vartheta}(\vartheta,\ \zeta;\ \varsigma) - 2\Upsilon(\vartheta,\ \zeta;\ \varsigma) + 3\Upsilon^2(\vartheta,\ \zeta;\ \varsigma) = 0,\ 0 < \rho \le 1, \\ \\ \Upsilon(\vartheta,\ 0;\ \varsigma) = \alpha\Lambda(\varsigma), \end{cases} \tag{28}$$

where $\Lambda(\varsigma) = [\underline{\Lambda}(\varsigma),\ \overline{\Lambda}(\varsigma)] = [\varsigma - 1,\ 1 - \varsigma]$, $\varsigma \in [0,\ 1]$ is a fuzzy number.

The parametric form of (28) is shown as:

$$\begin{cases} \mathfrak{D}_{\zeta}^{\rho}\underline{\Upsilon}(\vartheta,\ \zeta;\ \varsigma)-\underline{\Upsilon}_{\vartheta\vartheta}(\vartheta,\ \zeta;\ \varsigma)-2\underline{\Upsilon}(\vartheta,\ \zeta;\ \varsigma)+3\underline{\Upsilon}^2(\vartheta,\ \zeta;\ \varsigma)=0,\\ \underline{\Upsilon}(\vartheta,\ 0;\ \varsigma)=(\varsigma-1)\alpha,\\ \mathfrak{D}_{\zeta}^{\rho}\overline{\Upsilon}(\vartheta,\ \zeta;\varsigma)-\overline{\Upsilon}_{\vartheta\vartheta}(\vartheta,\ \zeta;\ \varsigma)-2\overline{\Upsilon}(\vartheta,\ \zeta;\ \varsigma)+3\overline{\Upsilon}^2(\vartheta,\ \zeta;\ \varsigma)=0,\\ \overline{\Upsilon}(\vartheta,\ 0;\ \varsigma)=(1-\varsigma)\alpha. \end{cases} \tag{29}$$

Applying the LT tool into (29) yields:

$$\begin{aligned} &\underline{\Psi}(\vartheta,\ \omega;\ \varsigma)-(\varsigma-1)\alpha\omega^{-1}-\omega^{-\rho}\underline{\Psi}_{\vartheta\vartheta}(\vartheta,\ \omega;\ \varsigma)-2\omega^{-\rho}\underline{\Psi}(\vartheta,\ \omega;\ \varsigma)+3\omega^{-\rho}\mathbb{L}\left\{\mathbb{L}^{-1}\left[\underline{\Psi}^2(\vartheta,\ \omega;\ \varsigma)\right]\right\}=0,\\ &\overline{\Psi}(\vartheta,\ \omega;\ \varsigma)-(1-\varsigma)\alpha\omega^{-1}-\overline{\Psi}_{\vartheta\vartheta}(\vartheta,\ \omega;\ \varsigma)-2\omega^{-\rho}\overline{\Psi}(\vartheta,\ \omega;\ \varsigma)+3\omega^{-\rho}\mathbb{L}\left\{\mathbb{L}^{-1}\left[\overline{\Psi}^2(\vartheta,\ \omega;\ \varsigma)\right]\right\}=0. \end{aligned} \tag{30}$$

According to L-FRPS method, we seek the solutions of the system $\lim_{\omega\to\infty}\omega^{j\rho+1}\mathbb{L}\left\{\mathrm{Res}^j\left(\underline{\Psi}^j(\vartheta,\ \omega;\ \varsigma)\right)\right\}=0$, and $\lim_{\omega\to\infty}\omega^{j\rho+1}\mathbb{L}\left\{\mathrm{Res}^j\left(\overline{\Psi}^j(\vartheta,\ \omega;\ \varsigma)\right)\right\}=0$, such that

$$\begin{aligned} \omega^{j\rho+1}\mathbb{L}\left\{\mathrm{Res}^j\left(\underline{\Psi}^j(\vartheta,\ \omega;\ \varsigma)\right)\right\}&=(\varsigma-1)\Bigg(\gamma_j(\vartheta)-2\gamma_{j-1}(\vartheta)-\gamma_{j-1}''(\vartheta)\\ &\quad+3\Gamma((j-1)\rho+1)\sum_{i=0}^{j-1}\frac{\gamma_i(\vartheta)\gamma_{j-i-1}(\vartheta)}{\Gamma(i\rho+1)\Gamma((j-i-1)\rho+1)}\Bigg),\\ \omega^{j\rho+1}\mathbb{L}\left\{\mathrm{Res}^j\left(\overline{\Psi}^j(\vartheta,\ \omega;\ \varsigma)\right)\right\}&=(1-\varsigma)\Bigg(\delta_j(\vartheta)-2\delta_{j-1}(\vartheta)-\delta_{j-1}''(\vartheta)\\ &\quad+3\Gamma((j-1)\rho+1)\sum_{i=0}^{j-1}\frac{\delta_i(\vartheta)\delta_{j-i-1}(\vartheta)}{\Gamma(i\rho+1)\Gamma((j-i-1)\rho+1)}\Bigg). \end{aligned} \tag{31}$$

Then, by solving the obtained algebraic system (31) for $\gamma_j(\vartheta)$, and $\delta_j(\vartheta)$. One can reach the following recurrence relations for $j\geq 1$:

$$\begin{aligned} \gamma_j(\vartheta)&=2\gamma_{j-1}(\vartheta)+\gamma_{j-1}''(\vartheta)-3\Gamma((j-1)\rho+1)\sum_{i=0}^{j-1}\frac{\gamma_i(\vartheta)\gamma_{j-i-1}(\vartheta)}{\Gamma(i\rho+1)\Gamma(j-i-1)\rho+1)},\\ \delta_j(\vartheta)&=2\delta_{j-1}(\vartheta)+\delta_{j-1}''(\vartheta)-3\Gamma((j-1)\rho+1)\sum_{i=0}^{j-1}\frac{\delta_i(\vartheta)\delta_{j-i-1}(\vartheta)}{\Gamma(i\rho+1)\Gamma(j-i-1)\rho+1)}. \end{aligned} \tag{32}$$

Using the MATHEMATICA Software Package 12 and the obtained recurrence relation (32), we determine- the following first four unknown functions of the LFPSEs of (30), considering $\gamma_0(\vartheta) = \delta_0(\vartheta) = \alpha$:

$$\gamma_1(\vartheta;\, \varsigma) = \alpha(2-3\alpha(\varsigma-1))(\varsigma-1),$$

$$\gamma_2(\vartheta;\, \varsigma) = 2\alpha(1-3\alpha(\varsigma-1))(2-3\alpha(\varsigma-1))(\varsigma-1),$$

$$\gamma_3(\vartheta;\, \varsigma) = -\frac{1}{\Gamma^2(\rho+1)}\alpha(\varsigma-1)(3\alpha(\varsigma-1)-2)\left(4(1-3\alpha(\varsigma-1))^2\Gamma(\rho+1)^2+3\alpha(\varsigma-1)(3\alpha(\varsigma-1)-2)\Gamma(2\rho+1)\right),$$

$$\gamma_4(\vartheta;\, \varsigma) = \frac{1}{\Gamma^2(\rho+1)\Gamma(2\rho+1)}2\alpha(\varsigma-1)(9\alpha(\varsigma-1)(\alpha(\varsigma-1)-1)+2)\left(4(1-3\alpha(\varsigma-1))^2\Gamma(2\rho+1)\Gamma^2(\rho+1)\right.,$$

$$\left.+\,6\alpha(\varsigma-1)(3\alpha(\varsigma-1)-2)\Gamma(3\rho+1)\Gamma(\rho+1)+3\alpha(\varsigma-1)(3\alpha(\varsigma-1)-2)\Gamma^2(2\rho+1)\right),$$

and

$$\delta_1(\vartheta;\varsigma) = \alpha(2+3\alpha(1-\varsigma))(1-\varsigma),$$

$$\delta_2(\vartheta;\varsigma) = 2\alpha(1+3\alpha(1-\varsigma))(2+3\alpha(1-\varsigma))(1-\varsigma),$$

$$\delta_3(\vartheta;\varsigma) = -\frac{1}{\Gamma^2(\rho+1)}\alpha(\varsigma-1)(3\alpha(\varsigma-1)+2)\left(4(3\alpha(\varsigma-1)+1)^2\Gamma(\rho+1)^2+3\alpha(\varsigma-1)(3\alpha(\varsigma-1)+2)\Gamma(2\rho+1)\right),$$

$$\delta_4(\vartheta;\varsigma) = -\frac{1}{\Gamma^2(\rho+1)\Gamma(2\rho+1)}2\alpha(\varsigma-1)(9\alpha(\varsigma-1)(\alpha(\varsigma-1)+1)+2)\left(4(3\alpha(\varsigma-1)+1)^2\Gamma(2\rho+1)\Gamma^2(\rho+1)\right.,$$

$$\left.+\,6\alpha(\varsigma-1)(3\alpha(\varsigma-1)+2)\Gamma(3\rho+1)\Gamma(\rho+1)+3\alpha(\varsigma-1)(3\alpha(\varsigma-1)+2)\Gamma^2(2\rho+1)\right).$$

Moreover, the components $\gamma_j(\vartheta;\, \varsigma)$, and $\delta_j(\vartheta;\, \varsigma)$ for each $j \geq 5$ can be listed similarly. The gained j terms in the shape of an infinite series are then used to create the approximate solutions $\underline{\Psi}(\vartheta,\, \omega;\, \varsigma)$, $\overline{\Psi}(\vartheta,\, \omega;\, \varsigma)$ as follows:

$$\begin{aligned}\underline{\Psi}(\vartheta,\, \omega;\, \varsigma) =& \alpha(\varsigma-1)\omega^{-1}+\alpha(2-3\alpha(\varsigma-1))(\varsigma-1)\omega^{-\rho-1}\\ &+2\alpha(1-3\alpha(\varsigma-1))(2-3\alpha(\varsigma-1))(\varsigma-1)\omega^{-2\rho-1}-\frac{1}{\Gamma^2(\rho+1)}\alpha(\varsigma-1)(3\alpha(\varsigma-1)\\ &-2)\left(4(1-3\alpha(\varsigma-1))^2\Gamma(\rho+1)^2+3\alpha(\varsigma-1)(3\alpha(\varsigma-1)-2)\Gamma(2\rho+1)\right)\omega^{-3\rho-1}+\ldots,\end{aligned}$$

$$\overline{\Psi}(\vartheta,\ \omega;\ \varsigma) = \alpha(1-\varsigma)\omega^{-1} - \alpha(2+3\alpha(1-\varsigma))(1-\varsigma)\omega^{-\rho-1} - 2\alpha(1+3\alpha(1-\varsigma))(2+3\alpha(1-\varsigma))(1$$
$$-\varsigma)\omega^{-2\rho-1} - \frac{1}{\Gamma^2(\rho+1)}\alpha(\varsigma-1)(3\alpha(\varsigma-1)+2)\left(4(3\alpha(\varsigma-1)+1)^2\Gamma(\rho+1)^2 + 3\alpha(\varsigma)\right. \tag{33}$$
$$\left.-1)(3\alpha(\varsigma-1)+2)\Gamma(2\rho+1)\right)\omega^{-3\rho-1} + \ldots.$$

Consequently, the approximate series solutions $\underline{\Upsilon}(\vartheta,\ \zeta;\ \varsigma)$, and $\overline{\Upsilon}(\vartheta,\ \zeta;\ \varsigma)$ for the parametric form, fractional IVPs (29) can be provided as

$$\begin{aligned}
\underline{\Upsilon}(\vartheta,\ \zeta;\ \varsigma) =& \alpha(\varsigma-1)\left(1+(2-3\alpha(\varsigma-1))\frac{\zeta^\rho}{\Gamma(\rho+1)} + 2(1-3\alpha(\varsigma-1))(2-3\alpha(\varsigma-1))\frac{\zeta^{2\rho}}{\Gamma(2\rho+1)} - (3\alpha(\varsigma)\right.\\
&-1)-2)\left(4(1-3\alpha(\varsigma-1))^2\Gamma(\rho+1)^2 + 3\alpha(\varsigma-1)(3\alpha(\varsigma-1)-2)\Gamma(2\rho\ ,\right.\\
&\left.\left.+1)\right)\frac{\zeta^{3\rho}}{\Gamma(3\rho+1)\Gamma^2(\rho+1)}\right) + \ldots,\\
\overline{\Upsilon}(\vartheta,\ \zeta;\ \varsigma) =& \alpha(1-\varsigma)\left(1-(2+3\alpha(1-\varsigma))\frac{\zeta^\rho}{\Gamma(\rho+1)} - 2(1+3\alpha(1-\varsigma))(2+3\alpha(1-\varsigma))\frac{\zeta^{2\rho}}{\Gamma(2\rho+1)}\right.\\
&+(3\alpha(\varsigma-1)+2)\left(4(3\alpha(\varsigma-1)+1)^2\Gamma(\rho+1)^2\right.\\
&\left.\left.+3\alpha(\varsigma-1)(3\alpha(\varsigma-1)+2)\Gamma(2\rho+1)\right)\frac{\zeta^{3\rho}}{\Gamma(3\rho+1)\Gamma^2(\rho+1)}\right) + \ldots.
\end{aligned} \tag{34}$$

Especially, the acquired approximate solutions of fractional IVPs (29) at $\rho = 1$ can be formulated as:

$$\begin{aligned}
\underline{\Upsilon}(\vartheta,\ \zeta;\ \varsigma) =& -\frac{1}{3}\alpha(-3+\zeta(3+\zeta(3+\zeta(2+9\alpha(-2+3\alpha(\varsigma-1))(\varsigma-1))-9\alpha(\varsigma-1)))\\
&(-2+3\alpha(\varsigma)-1))(\varsigma-1)+\ldots,\\
\overline{\Upsilon}(\vartheta,\ \zeta;\ \varsigma) =& \alpha\left(1-\frac{1}{3}\zeta(3+\zeta(3+\zeta(2+9\alpha(2+3\alpha(\varsigma-1))(\varsigma-1))+9\alpha(\varsigma-1)))(2+3\alpha(\varsigma-1))(\varsigma-1)-\varsigma\right)+\ldots,
\end{aligned} \tag{35}$$

which is in accordance with the findings of [29] and aligns with the Taylor series of the exact solutions $\underline{\Upsilon}(\vartheta,\ \zeta;\ \varsigma) = (\varsigma-1)\dfrac{\left(-\frac{2}{3}\right)\alpha e^{2\zeta}}{\left(-\frac{2}{3}\right)+\alpha\left(1-e^{2\zeta}\right)}$, and $\overline{\Upsilon}(\vartheta,\ \zeta;\ \varsigma) = (1-\varsigma)\dfrac{\left(-\frac{2}{3}\right)\alpha e^{2\zeta}}{\left(-\frac{2}{3}\right)+\alpha\left(1-e^{2\zeta}\right)}$, at $\rho = 1$.

Absolute errors at sufficient grid points in the interval $\zeta \in [0, 2]$ between the fuzzy sixth approximate and exact solutions of the posed problem (28) at $\vartheta = 5$ when $\alpha = 0.001$ achieved using the L-FRPS algorithm are shown in Table 5. The effect of the recommended approach on the fuzzy lower and upper portions of $[\Upsilon(\vartheta, \zeta; \varsigma)]$, and $[\Upsilon_6(\vartheta, \zeta; \varsigma)]$ for Application 4.3 with various uncertain levels with $\alpha \in \{0.1, 0.01\}$ is shown in Figure 6. While Figure 7 illustrates the behavior of fuzzy lower and upper solutions $[\Upsilon(\vartheta, \zeta; \varsigma)]$, and $[\Upsilon_6(\vartheta, \zeta; \varsigma)]$ using the triangle shape to adhere to the fuzzy theory. Figure 8, show the 3D behavior fuzzy lower and upper layers of $[\Upsilon(\vartheta, \zeta; \varsigma)]$, and $[\Upsilon_6(\vartheta, \zeta; \varsigma)]$ for various values of ρ and at fixed the uncertain level.

Table 5. Absolute errors of the approximating $\underline{\Upsilon}_6(5, \zeta; \varsigma)$, and $\overline{\Upsilon}_6(5, \zeta; \varsigma)$ for Application 4.3, at $\alpha = 0.001$

ζ	$\underline{\Upsilon}_6(5, \zeta; \varsigma)$			
	$\varsigma = 0$	$\varsigma = 0.3$	$\varsigma = 0.6$	$\varsigma = 0.9$
0.32	5.08898×10^{-6}	3.02595×10^{-6}	1.42287×10^{-6}	2.7922×10^{-7}
0.64	2.63771×10^{-5}	1.55702×10^{-5}	7.24705×10^{-6}	1.40003×10^{-6}
0.96	8.74468×10^{-5}	4.99831×10^{-5}	2.21654×10^{-5}	3.94746×10^{-6}
1.28	1.90435×10^{-4}	9.76473×10^{-5}	3.55093×10^{-5}	3.82662×10^{-6}
1.6	2.00094×10^{-4}	4.32644×10^{-5}	3.03155×10^{-5}	2.12694×10^{-5}
1.92	3.34454×10^{-4}	4.65872×10^{-4}	3.97904×10^{-4}	1.32215×10^{-4}
	$\overline{\Upsilon}_6(5, \zeta; \varsigma)$			
0.32	7.55402×10^{-9}	5.28643×10^{-7}	6.07428×10^{-7}	2.28254×10^{-13}
0.64	1.02657×10^{-6}	2.14253×10^{-6}	2.86252×10^{-6}	1.12599×10^{-7}
0.96	1.85284×10^{-5}	1.94443×10^{-6}	5.20963×10^{-6}	2.88772×10^{-6}
1.28	1.45095×10^{-4}	6.67603×10^{-5}	1.81743×10^{-5}	4.71383×10^{-6}
1.6	7.08817×10^{-4}	4.02094×10^{-4}	1.75737×10^{-4}	3.03582×10^{-5}
1.92	2.50698×10^{-3}	1.53039×10^{-3}	7.45497×10^{-4}	1.53941×10^{-4}

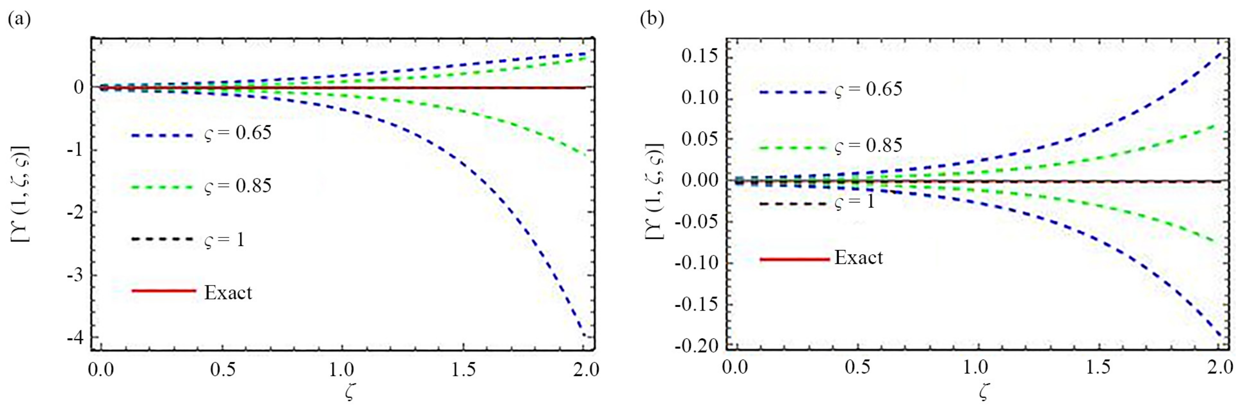

Figure 6. Plots of fuzzy lower and upper portions for Application 4.3; (a) $[\Upsilon(\vartheta, \zeta; \varsigma)]$, and $[\Upsilon_6(\vartheta, \zeta; \varsigma)]$ at $\alpha = 0.1$; (b) $[\Upsilon(\vartheta, \zeta; \varsigma)]$, and $[\Upsilon_6(\vartheta, \zeta; \varsigma)]$ at $\alpha = 0.01$

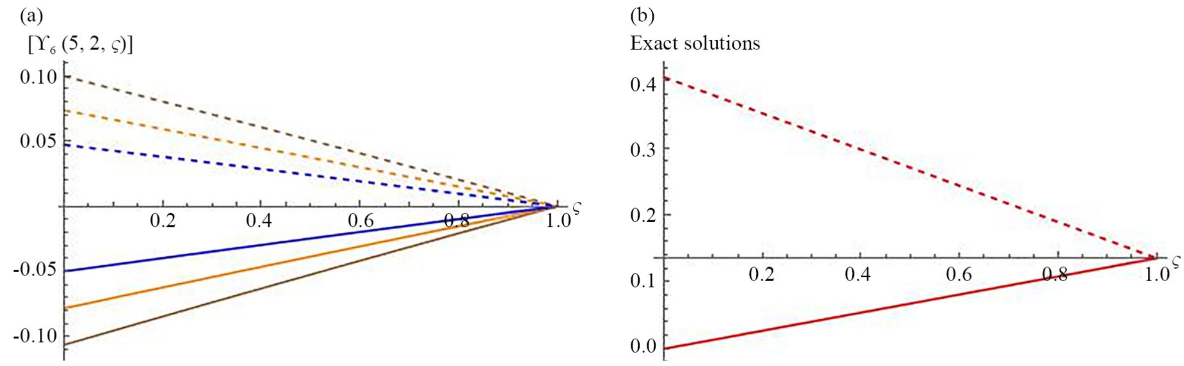

Figure 7. Plots of triangle fuzzy solutions at fixed values $\vartheta = 5$, and $\zeta = 0.2$; (a) $[\Upsilon_6(\vartheta,\ \zeta;\ \varsigma)]; \rho \in \{0.75,\ 0.85,\ 1\}$; (b) Exact solutions

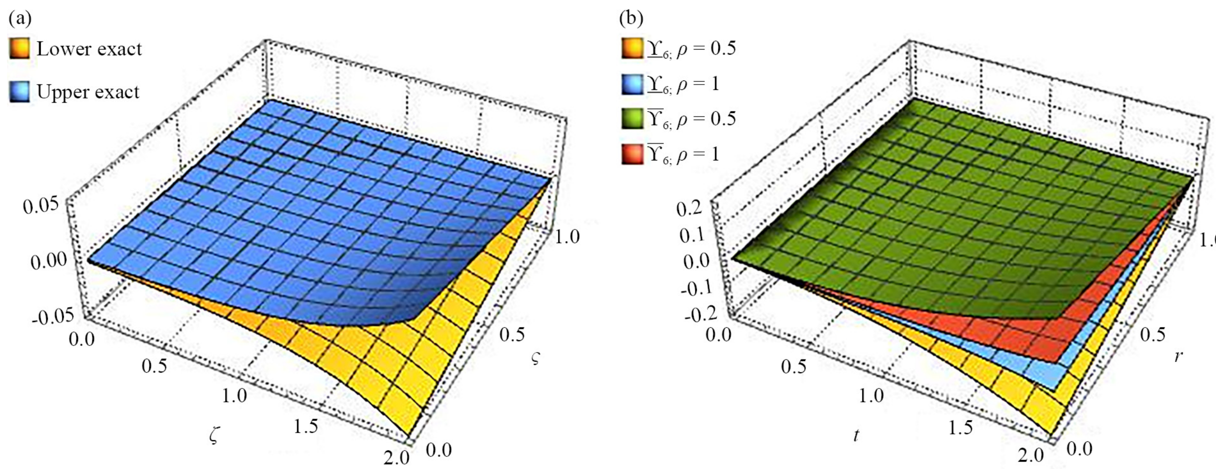

Figure 8. Surface behavior of findings for Application 4.3; (a) Fuzzy lower and upper exact solutions; (b) $\underline{\Upsilon}_6(1,\ \zeta;\ \varsigma)$, and $\overline{\Upsilon}_6(1,\ \zeta;\ \varsigma)$ when $\rho = 0.5$, and $\rho = 1$

5. Concluding remarks

This investigation introduces the analytical study of the fuzzy L-FRPS technique for successful application in predicting and generating analytic-approximate series solutions of fuzzy fractional gas, fuzzy fractional advection, and fuzzy fractional Newell-Whitehead-Segel models in the sense of fuzzy Caputo FD. The proper procedure has been established to create fractional approximate solutions of the considered uncertain models, along with fuzzy initial data via simulation of the FRPS strategy and the fuzzy LT operator in the Laplace domain under $(i - g\mathcal{H})$-differentiability. The suggested scheme's main advantages are its straightforwardness, quickness, and accuracy in discovering exact and accurate approximate series solutions of both linear and nonlinear fuzzy FODEs. To verify the validity of the proposed method. Our findings were simulated using 2D and 3D graphs for various values of FD order. From these depictions, the observed behavior of the lower bound as a rising function and the upper bound as a decreasing one indicates that the obtained solutions represent fuzzy numbers. Also, by altering the fractional order values, we conducted a parametric test to assess resilience. As the fractional order becomes closer to unity, the accuracy of the findings produced by the suggested method improves, as shown by the error analysis. These results validate the scheme's dependability and stability in the context of order changes. Additionally, we retrieve the fractional-order model's outcomes for the studied Applications as shown in [30–32] when we replace the uncertain level $\varsigma = 1$ in numerical solutions of the problems posed. Therefore, the global dynamic of the studied model is provided by the FD operator with fuzziness, as opposed to the traditional integer and fractional-order models. Consequently, the outcome declared that FC, in conjunction with fuzzy concepts, improves the dynamics of a physical process. In a future study, we may extend the L-FRPSM framework to interval-valued fuzzy uncertainty and trapezoidal fuzzy numbers for certain non-linear FFOPDEs. Further, we may also highlight possible extensions of the proposed method for exploring fuzzy approximate solutions of nonlinear control systems.

Conflict of interest

The authors declare no competing financial interest.

References

[1] Meral FC, Royston TJ, Magin R. Fractional calculus in viscoelasticity: An experimental study. *Communications in Nonlinear Science and Numerical Simulation*. 2010; 15(4): 939-945. Available from: https://doi.org/10.1016/j.cnsns.2009.05.004.

[2] Magin R, Ortigueira MD, Podlubny I, Trujillo J. On the fractional signals and systems. *Signal Processing*. 2011; 91(3): 350-371. Available from: https://doi.org/10.1016/j.sigpro.2010.08.003.

[3] Lakshmikantham V, Leela S, Devi JV. *Theory of Fractional Dynamic Systems*. Cambridge: Cambridge Scientific Publishers; 2009.

[4] Miller KS, Ross B. *An Introduction to Fractional Calculus and Differential Equations*. New York: Wiley; 1993.

[5] Deng L, Ducrot A. Existence of multi-dimensional pulsating fronts for KPP equations: A new formulation approach. *Calculus of Variations and Partial Differential Equations*. 2023; 62(4): 134. Available from: https://doi.org/10.1007/s00526-023-02473-y.

[6] Massoun Y, Alomari AK, Cesarano C. Analytic approach solution to time-fractional Phi-4 equation with two-parameter fractional derivative. *Fractal and Fractional*. 2024; 8(10): 576. Available from: https://doi.org/10.3390/fractalfract8100576.

[7] Alomari AK, Abdeljawad T, Baleanu D, Saad KM, Al-Mdallal QM. Numerical solutions of fractional parabolic equations with generalized Mittag-Leffler kernels. *Numerical Methods for Partial Differential Equations*. 2024; 40(1): e22699. Available from: https://doi.org/10.1002/num.22699.

[8] Shah R, Khan H, Baleanu D, Kumam P, Arif M. A novel method for the analytical solution of fractional Zakharov-Kuznetsov equations. *Advances in Difference Equations*. 2019; 517: 1. Available from: https://doi.org/10.1186/s13662-019-2441-5.

[9] Zadeh LA. Fuzzy sets as a basis for a theory of possibility. *Fuzzy Sets and Systems*. 1978; 100(1): 3-28. Available from: https://doi.org/10.1016/S0165-0114(99)80004-9.

[10] Zadeh LA, Chang SL. On fuzzy mapping and control. *IEEE Transactions on Systems, Man, and Cybernetics*. 1972; SMC-2(1): 30-34. Available from: https://doi.org/10.1109/TSMC.1972.5408553.

[11] Zadeh LA. The concept of a linguistic variable and its application to approximate reasoning-I. *Information Sciences*. 1975; 8(3): 199-249. Available from: https://doi.org/10.1016/0020-0255(75)90036-5.

[12] Zadeh LA. Linguistic variables, approximate reasoning, and dispositions. *Medical Informatics*. 1983; 8(3): 173-186. Available from: https://doi.org/10.3109/14639238309016081.

[13] Zadeh LA, Klir GJ, Yuan B. *Fuzzy Sets, Fuzzy Logic, and Fuzzy Systems: Selected Papers*. Vol. 6. Singapore: World Scientific; 1996. Available from: https://doi.org/10.1142/2895.

[14] Stefanini L. A generalization of Hukuhara difference and division for interval and fuzzy arithmetic. *Fuzzy Sets and Systems*. 2010; 161(11): 1564-1584. Available from: https://doi.org/10.1016/j.fss.2009.06.009.

[15] Chalco-Cano Y, Rufián-Lizana A, Román-Flores H, Jiménez-Gamero MD. Calculus for interval-valued functions using generalized Hukuhara derivative and applications. *Fuzzy Sets and Systems*. 2013; 219: 49-67. Available from: https://doi.org/10.1016/j.fss.2012.12.004.

[16] Alaroud M, Ahmad RR, Din UKS. An efficient analytical-numerical technique for handling model of fuzzy differential equations of fractional-order. *Filomat*. 2019; 33(2): 617-632. Available from: https://doi.org/10.2298/FIL1902617A.

[17] Agarwal RP, Lakshmikantham V, Nieto JJ. On the concept of solution for fractional differential equations with uncertainty. *Nonlinear Analysis: Theory, Methods & Applications*. 2010; 72(6): 2859-2862. Available from: https://doi.org/10.1016/j.na.2009.11.029.

[18] Arshad S, Lupulescu V. On the fractional differential equations with uncertainty. *Nonlinear Analysis: Theory, Methods & Applications*. 2011; 74(11): 3685-3693. Available from: https://doi.org/10.1016/j.na.2011.02.048.

[19] Salahshour S, Ahmadian A, Chan CS, Baleanu D. Toward the existence of solutions of fractional sequential differential equations with uncertainty. In: *2015 IEEE International Conference on Fuzzy Systems (FUZZ-IEEE)*. Istanbul, Turkey: IEEE; 2015. p.1-6. Available from: https://doi.org/10.1109/FUZZ-IEEE.2015.7338013.

[20] Long HV, Son NTK, Tam HTT. The solvability of fuzzy fractional partial differential equations under Caputo gH-differentiability. *Fuzzy Sets and Systems*. 2017; 309: 35-63. Available from: https://doi.org/10.1016/j.fss.2016.06.018.

[21] Salahshour S, Allahviranloo T, Abbasbandy S. Solving fuzzy fractional differential equations by fuzzy Laplace transforms. *Communications in Nonlinear Science and Numerical Simulation*. 2012; 17(3): 1372-1381. Available from: https://doi.org/10.1016/j.cnsns.2011.07.005.

[22] Allahviranloo T, Salahshour S, Abbasbandy S. Explicit solutions of fractional differential equations with uncertainty. *Soft Computing*. 2012; 16(2): 297-302. Available from: https://doi.org/10.1007/s00500-011-0743-y.

[23] Osman M, Xia Y, Omer OA, Hamoud A. On the Fuzzy solution of linear-nonlinear partial differential equations. *Mathematics*. 2022; 10(13): 2295. Available from: https://doi.org/10.3390/math10132295.

[24] Štepnicka M, Valášek R. Fuzzy transforms and their application to wave equation. *Journal of Electrical Engineering*. 2004; 55(12): 7-10.

[25] Gouyandeh Z, Allahviranloo T, Abbasbandy S, Armand A. A fuzzy solution of heat equation under generalized Hukuhara differentiability by fuzzy Fourier transform. *Fuzzy Sets and Systems*. 2017; 309: 81-97. Available from: https://doi.org/10.1016/j.fss.2016.04.010.

[26] Ullah A, Ullah A, Ahmad S, Ahmad I, Akgül A. On solutions of fuzzy fractional order complex population dynamical model. *Numerical Methods for Partial Differential Equations*. 2023; 39(6): 4595-4615. Available from: https://doi.org/10.1002/num.22654.

[27] Allahviranloo T, Ghobadi M, Matinfar M. A fuzzy solution of wave equation by FFS-transform. *Numerical Methods for Partial Differential Equations*. 2024; 40(1): e22661. Available from: https://doi.org/10.1002/num.22661.

[28] Saeed NA, Pachpatte DB. Usage of the fuzzy Adomian decomposition method for solving some fuzzy fractional partial differential equations. *Advances in Fuzzy Systems*. 2024; 2024: 8794634. Available from: https://doi.org/10.1155/2024/8794634.

[29] Alkhezi Y, Shah NA, Ntwiga DB. Analytical fuzzy analysis of a fractional-order Newell-Whitehead-Segel model with Mittag-Leffler Kernel. *Journal of Function Spaces*. 2022; 2022: 2785379. Available from: https://doi.org/10.1155/2022/2785379.

[30] Wazwaz AM. *Partial Differential Equations and Solitary Waves Theory*. Berlin: Springer; 2010. Available from: https://doi.org/10.1007/978-3-642-00251-9.

[31] Alaroud M, Ababneh O, Tahat N, Al-Omari S. Analytic technique for solving temporal time-fractional gas dynamics equations with Caputo fractional derivative. *AIMS Mathematics*. 2022; 7(10): 17647-17669. Available from: https://doi.org/10.3934/math.2022972.

[32] Kumar D, Sharma RP. Numerical approximation of the Newell-Whitehead-Segel equation of fractional order. *Nonlinear Engineering*. 2016; 5(2): 81-86. Available from: https://doi.org/10.1515/nleng-2015-0032.

[33] He JH, Wu XH. Variational iteration method: New development and applications. *Computers & Mathematics with Applications*. 2007; 54(7-8): 881-894. Available from: https://doi.org/10.1016/j.camwa.2006.12.083.

[34] Wu GC, He JH. Fractional Adomian decomposition method. *arXiv:1006.5264*. 2010. Available from: https://doi.org/10.48550/arXiv.1006.5264.

[35] Liao S. Homotopy analysis method: A new analytical technique for nonlinear problems. *Communications in Nonlinear Science and Numerical Simulation*. 1997; 2(2): 95-100. Available from: https://doi.org/10.1016/S1007-5704(97)90047-2.

[36] Dubois D, Prade H. Operations on fuzzy numbers. *International Journal of Systems Science*. 1978; 9(6): 613-626. Available from: https://doi.org/10.1080/00207727808941724. .

[37] Malomed B. The Newell-Whitehead-Segel equation for traveling waves. *arXiv:patt-sol/9605001*. 1996. Available from: https://doi.org/10.48550/arXiv.patt-sol/9605001.

[38] Emmons HW. *Fundamentals of Gas Dynamics*. Princeton: Princeton University Press; 2015.